A THESIS FOR THE DEGREE OF MASTER OF SCIENCE

Comparative analysis of selected superoxide dismutases (SODs) from big belly seahorse (*Hippocampus abdominalis*) and black rockfish (*Sebastes schlegelii*); revealing their putative significance in host antioxidant defense system

Narahenpitage Chathurika Nadeeshani Perera

DEPARTMENT OF MARINE LIFE SCIENCES

GRADUATE SCHOOL

JEJU NATIONAL UNIVERSITY

REPUBLIC OF KOREA

February 2017

Comparative analysis of selected superoxide dismutases (SODs) from big belly seahorse (*Hippocampus abdominalis*) and black rockfish (*Sebestes schlegelii*); revealing their putative significance in host antioxidant defense system

Narahenpitage Chathurika Nadeeshani Perera

(Supervised by Professor Jehee Lee)

A thesis submitted in partial fulfillment of the requirement for the degree of

MASTER OF SCIENCE

February 2017

The thesis has been examined and approved by

…………………………………………………………………………………

Thesis Director, **Qiang Wan**, Research Professor of Marine Life Sciences
Fish Vaccine Research Center, Jeju National University

…………………………………………………………………………………

Chulhong Oh, Associate Professor
Department of Marine Biology, University of Science and Technology, Rep. of Korea

…………………………………………………………………………………

Jehee Lee, Professor of Marine Life Sciences
School of Bio Medical Sciences, Jeju National University

Date:……………………………

DEPARTMENT OF MARINE LIFE SCIENCES
GRADUATE SCHOOL
JEJU NATIONAL UNIVERSITY
REPUBLIC OF KOREA

Every challenging work needs self-efforts as well as guidance of elders especially those who were very close to our heart.

My humble effort I dedicate to my ever loving

Mother and Father,

Whose affection, love, encouragement make me able to get such success.

Also, this dissertation is dedicated to my dearest husband who has been a great source of motivation, inspiration and backing through all these years

Acknowledgement

I would like to offer my first and foremost thanks and gratitude to my supervisor, Professor Jehee Lee, Jeju National University for his guidance, understanding, patience and most importantly his immense knowledge and professional experience during my graduate studies at the Marine Molecular Genetics Laboratory, Jeju National University, Jeju, Republic of Korea. The door to Prof. Jehee Lee office was always open whenever I ran into a trouble spot or had a question about my research or writing. He consistently allowed this paper to be my own work, but steered me in the right the direction whenever he thought I needed it. From finding an appropriate subject in the beginning to the process of writing thesis, he offers his unreserved help and guidance and led me to finish my thesis step by step. His mentorship was paramount in providing a well-rounded experience consistent my long-term career goals. He encouraged me not only to grow as an experimentalist but also to finish this dissertation academically while guiding me through the rough road as an independent thinker. During my study period in Jeju National University, I have adored him as a great advisor, good leader with goal-oriented personality. I am really grateful to have him in my enlighten event of my life.

Especially, I would like to extent my sincere thanks and give credit those members of my masters committee, Research Professor Qiang Wan and Associate Professor Chulhong Oh for their input, valuable discussions and accessibility. Also my gratitude goes for the other professors in my department for their expertise, patience and conductive comments during my coursework.

I remember the generosity and encouragement of past and present colleagues of our laboratory and I am thankful to all of them for their valuable help in research work as well as in numerous ways in my life in Korea who have given me their unequivocal support throughout, as always, for which my mere expression of thanks likewise does not suffice. Further, I am also grateful to Department of Marine Life Sciences for providing me a peaceful environment for my academic and research works. I praise the enormous amount of help and teachings to all those whom I have not mentioned above but helped me in numerous ways to my success.

My warmest gratitude goes to my mother, father and brother for their love, care, moral support and advice throughout my life.

Last but not least, I want to express my enormous gratitude to my ever loving husband, Gelshan Imarshana Godahewa for his priceless encouragement and unflagging love gave to me at every time. This successful dissertation is simply impossible without you.

Summary

Cellular redox processes such as oxidative phosphorylation may lead to excess electrons in solution. As cells have reasonable oxygen concentrations, superoxide radical ($O_2^{\bullet-}$) can be rapidly formed by attachment of the electron. Superoxide radical is not a particularly strong reductant or oxidant, so it is rather unreactive with the amino acids that comprise the protein backbone, with the notable exceptions of the sulfur-containing amino acids, cysteine and methionine. It is, however, very reactive with some transition metal complexes and the corresponding aquated ions, particularly copper, iron and manganese. Superoxide dismutases (SODs) are enzymes that function to catalytically convert $O_2^{\bullet-}$ to oxygen (O_2) and hydrogen peroxide (H_2O_2). Based on the metal co-factor they harbor, SODs can be classified into four groups: iron SOD (FeSOD), manganese SOD (MnSOD), copper-zinc SOD (CuZnSOD), and nickel SOD (NiSOD). The evolutionary reason for the separation of SODs with different metal requirements is probably related to the different availability of soluble transition metal compounds in the biosphere in relation to the O_2 content of the atmosphere in different geological eras.

Two intracellular types of SODs are known in mammalian cells, a mitochondrial, tetrameric manganese-containing enzyme (Mn-SOD) and a cytosolic, dimeric copper/ zinc-containing enzyme (Cu/Zn-SOD). Although these two SODs catalyze the same reaction, they have quite distinct structures and appear to be unrelated in terms of their evolution. SODs in primates have been studied mainly in humans, and to a much lesser extent in nonhuman primates. SODs have been found to be important for the long life-span of primates. The overall mechanism by which SODs function has been called a "ping-pong" mechanism as it involves the sequential reduction and oxidation of the metal center, with the concomitant oxidation and

reduction of superoxide radicals at virtually diffusion controlled rates that generally include a pH range where the rate is unchanging.

The main role of SODs in all aerobic organisms is to neutralize the $O_2^{\bullet-}$ produced in the cytosol, mitochondria and endoplasmic reticulum of cells. However, the SOD can also have a pro-oxidant effect because the dissociation of the $O_2^{\bullet-}$ produces H_2O_2, which is toxic to cells. It is to remove this dangerous H_2O_2 that the presence of others antioxidant systems, such as CAT and GPx enzymes, becomes necessary.

In this study, four SOD genes including the CuZnSOD and MnSOD, each from big belly seahorse and rockfish have been identified and characterized at molecular and functional level. This report is divided into three main chapters based on the two different species and metal cofactors.

In chapter I, seahorse CuZnSOD and rockfish CuZnSOD were characterized at molecular level while analyzing their functional characteristics features and transcriptional modulation under pathological conditions. The complete cDNA sequences of ShCuZnSOD and RfCuZnSOD were consisted of 842 bp and 853 bp, respectively. Their putative polypeptide sequences were 154 aa (15.94 kDa) and 154 aa (16.04 kDa), respectively. Subsequently, the identified sequences were characterized using various bioinformatics tools, while comparing the sequences with other known similitudes. Both ShCuZnSOD and RfCuZnSOD shared similar domain architecture including putative *N*-glycosylation sites, a typical Cu/Zn_SOD domain, two signature motifs and three cysteine residues. ShCuZnSOD and RfCuZnSOD shared highest identity with *Siniperca chuatsi* (87.7%) and *Lates calcarifer* (87 %), respectively. Phylogenetic analysis revealed that both ShCuZnSOD and RfCuZnSOD were tightly clustered with the fish clade. The antioxidant function of ShCuZnSOD and RfCuZnSOD in the antioxidant system was evaluated *via* the xanthine/XOD assay. The highest activity of rShCuZnSOD was observed at pH 9; where the optimum pH for the rRfCuZnSOD was pH 8. The highest activity was recorded at 25 °C for both rCuZnSODs. According to the results the SOD activity was increased with the increasing concentration of both rCuZnSODs. rMBP did not have a significant impact on antioxidant activity. KCN, DDC, and NaN_3 showed significant effects on the relative activity of both rCuZnSODs but EDTA had no effect. The peroxidation function of both rShCuZnSOD and rRfCuZnSOD were assessed by investigating cell viability using an MTT assay. Cell viability increased in the presence of HCO_3^- and rCuZnSODs in a dose dependent manner; the highest percentages were observed in the 100 µg/mL of rCuZnSODs, which resulted in ~73% increase in rShCuZnSOD and ~ 68% in rRfCuZnSOD. Extracellular H_2O_2 scavenging activity of rShCuZnSOD and rRfCuZnSOD in the presence of HCO_3^-, and the level of intracellular H_2O_2 in THP-1 cells were measured by flow cytometry. Intracellular ROS levels in the cells fell drastically after 100 µg/mL of rCuZnSOD (both rShCuZnSOD and rRFCuZnSOD) although the cells were exposed to oxidative stress by H_2O_2. The mRNA both *ShCuZnSOD* and *RfCuZnSOD* were significantly expressed in blood. In addition, both *ShCuZnSOD* and *RfCuZnSOD* were transcriptionally responded to immune challenges.

Chapter II enlightened the molecular characteristics and transcriptional properties of ShMnSOD and RfMnSOD. The complete cDNA sequence of ShMnSOD and RfMnSOD consisted of 1021 bp and 1061 bp, repectively. Two conservative domains including; Iron/Manganese SOD, C-terminal domain and Iron/Manganese SOD (SOD Fe-C domain), N-terminal domain (SOD Fe-N domain) were detected *via* the motif scan analyzer from both ShMnSOD and RfMnSOD.

Clustal W pairwise alignment revealed the highest identity and similarity of ShMnSOD with *Opleganathus fasciatus* MnSOD (91.6% and 94.2% respectively) and RfMnSOD with *Oplegnathus faciatus* (97.3% and 99.6% repectively). The highest activity of rShMnSOD in scavenging superoxide radicals was observed at pH 9. Contritely, the highest SOD activity of rRfMnSOD was observed at pH 8. The optimum temperature for its SOD activity of both rMnSODs was recorded at 25 ºC. Moreover, the activity of both rMnSODs increased while increasing the concentration of rMnSODs revealing their dose dependency. The highest inhibition was observed with the incubation of KCN and followed by NaN_3 for both rShMnSOD and rRfMnSOD. A constitutive expression of *ShMnOSD* and *RfMnSOD* with variable levels was observed in all fourteen tissues examined in the tissue specific expressional analysis. The highest expression was observed in the ovary and then followed by heart and brain in *ShMnSOD*. However, the highest expression of *RfMnSOD* was observed in blood and followed by ovary and skin. Additionally, both *ShMnSOD* and *RfMnSOD* mRNA were showed significant inductions against to immune stimulants used in the experiment. Third chapter describes the featured structural and functional variations of CuZnSOD and MnSOD of two different species.

Table of Content

List of Figures

List of Tables

1. Introduction

1.1 General introduction

As the human population continues to grow, finding means to feed those people are one of the most important challenges faced around the globe. Healthy diet, high in protein is necessary to ensure that growing population does not succumb to sickness and disease. Fish and other aquatic organisms are a great fit as a model for the important sources of food, nutrition, income and livelihoods for hundred millions of people around the world. Therefore, it has been already confirmed that the aquaculture is the fastest-growing food-production sector in the world, now providing almost half of the global fish supply. On the other hand ornamental fish culture is fast emerging as a major branch of aquaculture globally. Aquarium keeping is the second largest hobby in the world next to photography where the ornamental fish and aquatic plant industry is fast gaining importance due to its tremendous economic opportunities and prospects.

1.2 Reactive oxygen species and Antioxidants

It is a great challenge to rare the farm animals in a world that is highly populated with pathogenic microbes, massive range of toxic and allergenic substances that can be a threat for their physiological homeostasis. These may cause the stress which may produce hazardous reactive oxygen species (ROS) inside the hosts. Oxidative stress can simply define as the imbalance between oxidant exposure and antioxidant protection [1]. ROS that cause oxidative stress can be generated as by-products during mitochondrial electron transport, and as necessary intermediates of metal catalyzed oxidation reactions, including; superoxide anion (O^{2-}), hydroxyl radical ($OH^{\cdot}$), singlet oxygen ($O_2^{\cdot-}$) and hydrogen peroxide (H_2O_2). Activation of the phagocytic cells also can stimulate the production of ROS [2] which is called as respiratory burst. Highly reactive unpaired electron of these ROS can cause direct cellular injuries *via* inducing the lipid and protein peroxidation and damaging nucleic acids [3]. However, once the life has begun on the earth with the oxygen a large amount of antioxidant systems also inevitably adapted through the evolution. The productions of antioxidants are one of the means by which cells attempt to detoxify hazardous ROS [4] to limit the damage caused. Living organisms possess a variety of enzymatic and non-enzymatic antioxidant defense mechanisms that protect against the constant oxidative challenge by ensuring a proper balance between pro-oxidants and antioxidants. According to a previous report [4] the cellular antioxidant defenses can be categorized as primary (including antioxidant enzymes and small antioxidant molecules) and secondary defense systems (including proteolytic and lipolytic enzymes and the DNA repair systems).

1.3 Superoxide dismutases (SODs)

Superoxide dismutases (SODs) comprise a large family of such enzymatic antioxidants which are well-known metalloenzymes that catalyze the dismutation of superoxide into oxygen and hydrogen peroxide [5]. Depending on their metal content, they are classified into four groups: copper-zinc SOD (CuZnSOD), manganese SOD (MnSOD), iron SOD (FeSOD), and nickel SOD (NiSOD). FeSODs are mainly found in prokaryotes and plants, whereas NiSODs are predominant in bacteria. MnSODs are generally found in prokaryotes and the mitochondria of eukaryotes. CuZnSODs are found in the cytosol and extracellular compartments of eukaryotic cells and in the periplasm of Gram-negative bacteria [6]. This group is generally considered as the most important group of SOD because of their physiological and therapeutic importance [7].

1.4 Seahorse and Rockfish

Mainly in the industrialized countries it is a hobby to rare ornamental fish thus, the ornamental fish industry produces a luxury items and it will provide valuable income for developing nations as well [8]. Seahorses are one of the main types of ornamental fish specimens whom have the combined effect of demand on both ornamental trade and in traditional Chinese medicine. The big-belly seahorse (*Hippocampus abdominalis*) is one of the largest seahorse species; it is popular in the aquarium industry and is used for traditional medicine in Asia. Unlike other aquaculture species, seahorses generally do not adapt to harsh conditions causing them to be more vulnerable to infections. This species is also listed in Appendix II by CITES (Convention on International Trade in Endangered Species of Wild Fauna and Flora). Although some studies have reported on different aspects of the biology of this species including its feeding and growth, little information is available on its immunological characteristics. Also, culturing seahorses are quiet difficult than to the other aqua crops as they are more susceptible to the infections.

Rockfish (*Sebastes schlegelii*) is a highly demanded, economically important delicacy, particularly in the Asian-Pacific region, which includes the Republic of Korea. Its production has rapidly increased and is second only to olive flounder production in the Republic of Korea. However, the prevalence of infectious diseases causes adverse effects to the marine aquaculture production of rockfish and limits the ability to achieve high-quality and high-quantity production. Therefore, infectious pathogen control via rockfish innate immunity may be a crucial factor for obtaining a satisfactory production.

1.5 Aims of this work

Here in, we have identified MnSOD from big belly seahorse (*Hippocamps abdominalis*) and characterized its structural and functional features. The aim of this present study is to explore the potential antioxidant functions of ShMnSOD and reveals its putative function in the immune reactions. Thus, we have overexpressed and purified the rShMnSOD and then the recombinant protein was subjected to the functional assays in order to explore its antioxidant functions. Additionally we have discovered its role in the immune defense system by elucidating its gene expression in healthy tissues and in immune challenged tissues with immune stimulants.

2. Methodology

2.1 Construction of cDNA databases

A seahorse cDNA sequence database was constructed using the 454 GS-FLX™ sequencing technique (Roche, USA). In brief, total RNA was extracted from blood, liver, kidney, gill, and spleen tissues of 18 seahorses. The extracted RNA was treated with the RNeasy Mini kit (Qiagen, USA) and the quality and quantity were evaluated using an Agilent 2100 Bioanalyzer (Agilent Technologies, Canada); an RNA integration score (RIN) of 7.1 was obtained. For construction of a seahorse transcriptomic library, the RNA was fragmented into an average size of 1147 bp using the Titanium 454 sequencing system (Roche, USA). Finally, the sequencing was performed on one-half of the picotiter plate on a Roche 454 GS-FLX™ DNA platform at Macrogen, Korea.

A black rockfish cDNA sequence database was created by 454 GS-FLX™ sequencing [9]. Total RNA was extracted from blood, liver, head kidney, gill, intestine, and spleen tissues of three black rockfish and purified using the RNeasy Mini Kit (Qiagen, USA) following the manufacturer's instructions. The extracted RNA was quantified and its purity was assessed using an Agilent 2100 Bioanalyzer (Agilent Technologies, Canada), and an RNA integration score of 7.1 was obtained. A rockfish transcriptomic library was constructed by using the fragmented RNA (~1147 bases) samples (Macrogen, Korea).

2.2 *In silico* profiling

Domain and the signature analyses of ShCuZnSOD, RfCuZnSOD, ShMnSOD and RfMnSOD were carried using the ExPASy PROSITE Database (http://prosite.expasy.org/) and Motif Scan (http://myhits.isb-sib.ch/cgibin/motif_scan). Putative cleavage sites of the signal peptide were retrieved using SignalP (http://www.cbs.dtu.dk/services/SignalP/). The MultiLoc tool (http://abi.inf.uni-tuebingen.de/Services/MultiLoc/) was used to predict the cellular location of these four peptides. Potential *N*-linked glycosylation sites were predicted using the NetNGlyc web server (http://www.cbs.dtu.dk/services/NetNGlyc/). Molecular mass, isoelectric point and instability index of the putative ShCuZnSOD, RfCuZnSOD, ShMnSOD and RfMnSOD proteins were calculated by the ProtParam tool on ExPASy (http://web.expasy.org/protparam/). For the prediction of cysteine sites in the ShCuZnSOD and RfCuZnSOD peptides, the DiANNA 1.1 web server (http://clavius.bc.edu/~clotelab/DiANNA/) was used. To analyze the homology and evolutionary relationships of the ShCuZnSOD, RfCuZnSOD, ShMnSOD and RfMnSOD with their respective orthologs of other species, we performed a multiple sequence alignment and phylogenetic analysis using ClustalW (http://www.ebi.ac.uk/Tools/msa/clustalw2/) and the Neighbor-Joining (NJ) method at MEGA (ver. 5.0), respectively. The tertiary structure of these peptides were predicted using I-TASSER (http://zhanglab.ccmb.med.umich.edu/I-TASSER/) and SWISS-MODEL (http://swissmodel.expasy.org/) protein modeling servers and visualized using PyMOL v1.5 software.

2.3 Preparation of the recombinant plasmid constructs

To investigate the antioxidant role of these four SODs, the cDNA fragments including the CDS were amplified using gene-specific primers (Table 1). The amplicons were then isolated from a 1% agarose gel using a Gel Purification Kit (Accuprep, Bioneer, Korea). The pMAL-c5X vector and the amplicon were digested with *EcoR*I and *Hind*III restriction enzymes (TaKaRa, Japan). The digested cDNA fragments and pMAL-c5X vectors were gel purified and ligated using Mighty Mix

DNA Ligation Kit (TaKaRa, Japan). Finally, the constructed vectors were transformed into *Escherichia coli* DH5α competent cells. The plasmid constructs were purified from bacterial cells and subjected to sequence verification (Macrogen, Korea). The recombinant vectors were transformed into ER2523 (NEB Express) competent cells for protein expression.

2.4 Over expression and purification of recombinant plasmids

Protein expression and purification were carried out as described in our previous study [10] with slight modifications. Briefly, the recombinant pMAL-c5x/ShCuZnSOD, pMAL-c5x/RfCuZnSOD, pMAL-c5x/ShMnSOD and pMAL-c5x/RfMnSOD constructs were expressed in a bacterial system as a fusion protein with a maltosebinding protein (MBP) tag and then purified seperately. After a preliminary experiment to identify optimum conditions, the ER2523 cells were grown in LB broth (500 mL) supplemented with 100 mg mL^{-1} ampicillin and 100 mM glucose at 37 °C until the OD_{600} reached ~0.5. To induce protein expression, the culture was treated with 0.5 mM isopropyl-β-thiogalactopyranoside (IPTG) and shifted to 20 °C at 200 rpm with shaking for 10 h. The cells were harvested at 4000 × *g* for 20 min at 4 °C and the pelleted cells were resuspended in column buffer (20 mM Tris-HCl, pH 7.4, 200 mM NaCl) and stored at 20 °C overnight. On the following day, the cell suspension was thawed and lysed with lysozyme (1 mg mL^{-1}), followed by cold-sonication. The lysate was centrifuged (20,000 × *g* for 30 min at 4 °C), and the supernatant was passed through a column loaded with amylose resin (New England Biolabs) for affinity-binding. Amylose resins with the accumulated recombinant proteins were washed with column buffer (12 × volume). Finally, the respective proteins were eluted with elution buffer (column buffer + 10 mM maltose). The recombinant MBP (rMBP) was also overexpressed and purified using the same procedure and the concentration of recombinant proteins were assessed by a routine Bradford assay [11]. Samples obtained at different purification steps were subjected to 12% SDS-PAGE along with the molecular standards (Enzynomics, Korea). Coomassie blue R-250 (0.05%) was used to stain the gel, which was then de-stained by the standard procedure.

2.5 *In vitro* XOD/XO assay

A spectrophotometric method was used to investigate the antioxidant activity of rShCuZnSOD, rRfCuZnSOD, rShMnSOD and rRfMnSOD by the conventional xanthine/xanthine oxidase (xanthine/XOD) assay [12] as previously described [13]. Briefly, a reaction mixture containing 160 mL 0.1 M glycine-NaOH buffer (pH 9), 6.75 mL of each xanthine (3 mM), 3 mM EDTA (ethylenediaminetetraacetic acid), 0.15% BSA (bovine serum albumin), 0.75 mM NBT (nitro blue tetrazolium chloride), and 20 mL of rSOD proteins were separately prepared. The reaction mixture was incubated at 25 °C for 10 min and then the reaction was started by adding 6 mU of XOD and allowed to run for 20 min at 25 °C. OD_{560} was recorded using a microplate reader (Multiskan GO, Thermo Scientific). Two controls were run, namely, a positive control without any recombinant protein and a negative control with rMBP. All the experiments were conducted in triplicates and average values were obtained for statistical analyses. Maximum enzyme activity was defined as 100% in each assay. The following formulas were used to compute (a) inhibition percentage (I%) = [(Control OD_{560} - Test OD_{560})/Control OD_{560}] × 100, and (b) relative SOD activity (%) = (respective activity/highest activity) ×100.

2.5.1 *Effect of pH*

A xanthine/XOD assay was conducted under different pH conditions to evaluate the biophysical properties of above recombinant proteins. Enzyme samples were incubated in 0.1 M buffer at different pH values for 10 min. The optimum pH was determined by a pH gradient in different buffer systems, namely; citrate (pH 3, 4, 5), phosphate (pH 6, 7, 8) and glycine-NaOH (pH 9, 10, 11).

2.5.2 *Effect of temperature*

To determine the optimum temperature, a xanthine/XOD assay using 0.1 M glycine-NaOH buffer (pH 9) was conducted at different temperatures: 10, 20, 25, 30, 40, 50, 60, and 70 °C.

2.5.3 *Effect of concentration on activity*

Different doses (2.5, 5, 10, 20, 40, 80, and 160 µg) of rShCuZnSOD, rRfCuZnSOD, rShMnSOD, rRfMnSOD and rMBP were used in xanthine/XOD assays. Assays were performed at 25 °C using 0.1 M glycine-NaOH buffer (pH 9) and residual enzyme activity was determined.

2.5.4 *Effect of inhibitors*

The effects of four inhibitors on the antioxidant activity of these recombinant proteins were determined: potassium cyanide (KCN), dithiocarbamate (DDC), sodium azide (NaN_3), and EDTA. A concentration of 6.25 mM was used. The enzyme was incubated with an inhibitor at 25 °C in 0.1 M glycine-NaOH buffer (pH 9) for 15 min and residual enzyme activity was determined.

2.6 Peroxidation function analysis

2.6.1 *Cell viability assay*

A cell viability assay was performed to determine the ability of cells to maintain viability or to recover from oxidative stress in the presence or absence of the four rSODs. Human leukemia THP-1 cells (America Type Culture collection) were grown in RPMI 1640 culture medium in a 12-well plate. The culture medium was supplemented with 10% FBS, 100 U/mL penicillin and 100 mg/mL streptomycin and grown in a 5% CO_2 humidified incubator at 37 °C. The cells were exposed to different concentrations of rSODs (with and without metal supplementation) or rMBP with 20 mM $NaHCO_3$ for 30 min. They were then treated with 500 μmol H_2O_2 and incubated for 24 h at a density of 1×10^5 cells/mL. Eight experimental treatments were used in the assay with different concentration of recombinant proteins. The proportion of viable THP-1 cells was determined by a 3-(4,5-dimethylthiazol-2-yl)-2,5-diphenyl tetrazolium bromide (MTT) assay with slight modification of previously published protocols [14].

2.6.2 *ROS scavenging assay*

Fluorescence-activated cell sorting (FACS) was used to detect intracellular ROS levels in THP-1 cells. Briefly, THP-1 cells were grown in a 6-well plate (as described above) at 1×10^5 cells/mL. The cells were subjected to different concentrations of rSODs or rMBP with 20 mM $NaHCO_3$ for 30 min. Then, they were treated with 500 μmol H_2O_2 for 24 h. Ten different treatments were performed with different concentrations of recombinant protein. After 24 h, the cells were stained with 5 μmol H_2DCFDA for 30 min at 37 °C. Finally, intracellular ROS were detected by FACSCalibur flow cytometry (Becton Dickenson; San Jose, CA).

2.7 Animal husbandry

2.7.1 *Seahorse rearing and tissue isolation*

The healthy seahorse fish used in this study were purchased from the Korea Marine Ornamental Fish Breeding Center in Jeju Island (Republic of Korea). Fish (mean wt. 8 g) were stocked in laboratory aquarium tanks and allowed to acclimate for one week at laboratory conditions (temperature, 20 ± 1 °C) in aquarium tanks prior to the experiment. For the tissue distribution analysis, six seahorses (three male and three female) were used. Hematic cells were harvested after tail-cutting and the peripheral blood cells were separated by centrifugation at 3000 × *g* at 4 °C for 10 min. The tissue samples, including heart, gill, liver, spleen, kidney, intestine, stomach, skin, muscle, pouch, brain, testis, and ovary, were carefully dissected from the fish, snap frozen in liquid nitrogen and stored at 80 °C until analysis.

2.7.2 *Rockfish rearing and tissue isolation*

Healthy rockfish (200 ± 20 g) were obtained from the aquariums at the Marine Science Institute of Jeju National University (Jeju Self Governing Province, Republic of Korea) and were acclimatized to the laboratory conditions while maintaining them in 400 L laboratory aquarium tanks filled with aerated seawater at 22 ± 1 °C. For the tissue collection, five healthy rockfish were dissected aseptically. Initially, blood samples were taken (~1 mL) from each fish using sterile syringes coated with 0.2% heparin sodium salt (USB, USA), and hematic cells were immediately harvested by centrifugation at 3000 × *g* at 4 °C for 10 min. The other tissues, including the head kidney, spleen, liver, gill, intestine, kidney, muscle, skin, and heart, were carefully dissected from the fish, snap-frozen in liquid nitrogen, and stored at -80 °C until total RNA extraction.

2.8 Immune challenge experiment

2.8.1 *Seahorse*

Pre-acclimated healthy individuals were used to investigate the changes in tissue distribution of ShCuZnSOD and ShMnSOD after immunological challenge. Groups of seahorses were injected intraperitoneally with 100 µL of live pathogens including *Streptococcus iniae* (10^5 CFU/µL) or *Edwardsiella tarda* (5×10^3 CFU/µL), or with immune stimulants such as polyinosinic:polycytidylic acid (poly I:C; 1.5 µg/µL) or lipopolysaccharide (LPS; 1.25 µg/µL) in phosphate buffered saline. For the control group, 100 µL of PBS was injected. Seahorse peripheral blood cells were sampled from five individuals at 0, 3, 6, 12, 24, 48, and 72 h post-injection from each group. The aseptically collected samples were frozen in liquid nitrogen and stored at -80 °C.

2.8.2 *Rockfish*

In order to determine the transcriptional responses of RfCuZnSOD and RfMnSOD on viral or bacterial pathogens or stimulants, healthy rockfish were used for temporal transcriptional analysis. Each group of rockfish was injected intraperitoneally with polyinosinic:polycytidylic acid (poly I:C; 1.5 µg/µL, Sigma, USA), lipopolysaccharide (LPS; 1.25 µg/µL), and the gram-positive live bacterial pathogen *Streptococcus iniae* (1×10^5 colony-forming units/mL) after suspension in 1 phosphate buffered saline (PBS) in a total volume of 200 µL. Additionally, 200 µL of 1 × PBS was injected to the control group. For each treatment, blood cells and spleen tissues from five individuals were sampled at 0, 3, 6, 12, 24, 48, and 72 h after injection (p.i.), and samples were snap-frozen in liquid nitrogen and stored at -80 °C until total RNA extraction.

2.9 Total RNA extraction and first strand cDNA synthesis

Total RNAs from the pooled tissues used for tissue distribution of the proteins and immune challenged tissues were extracted using RNAiso plus (TaKaRa, Japan). The extracted total RNAs were purified using an RNeasy spin column (Qiagen, USA). RNA quality was determined by 1.5% agarose gel electrophoresis and concentration was determined at 260 nm in a µDrop Plate (Thermo Scientific, USA). Single-stranded cDNA was synthesized as described previously [15] using a PrimeScript II first strand cDNA synthesis kit (TaKaRa, Japan) with purified RNA samples (2.5 µg). The cDNA was diluted 1:40 and stored at -20 °C for subsequent quantitative real time PCR (qPCR) assays.

2.10 Quantitative real-time PCR (qPCR)

The expression patterns of ShCuZnSOD, RfCuZnSOD, ShMnSOD and RfMnSOD in different tissues were detected by qPCR using cDNA as the template and employing gene specific primers (Table 1). Seahorse 40S ribosomal protein S7 (Accession number KP780177) was used as the reference gene for *ShCuZnSOD* and *ShMnSOD* and rockfish elongation factor 1α (*RfEF1α*) gene as an internal reference (GenBank ID: KF430623) was used for the *RfCuZnSOD* and *RfMnSOD* which did not show any significant expressional variation within each tissue under same qPCR profile. To identify the transcriptional distribution of *ShCuZnSOD* and *ShMnSOD* blood, heart, gill, liver, spleen, kidney, intestine, stomach, skin, muscle, pouch, brain, testis, and ovary tissues were analyzed where instead of pouch, head kidney was used for *RfCuZnSOD* and *RfMnSOD*. Assays were performed in triplicate to increase the reliability of the results. For each amplification, a 10 µL reaction volume consisting of 3 µL diluted cDNA template, 5 µL 2× TaKaRa Ex Taq SYBR premix, 0.4 µL each forward and reverse primer (10 pmol/µL) and 1.2 µL of PCR grade H_2O was prepared. The amplification was performed using the following conditions: one cycle of 95 °C for 30 s, followed by 45 cycles of 95 °C for 5 s, 58 °C for 10 s and 72 °C for 20 s. Finally, a single cycle of 95 °C for 15 s, 60 °C for 30 s and 95 °C for 15 s was performed to construct a melting curve to evaluate the specificity of the primer pair. The Livak method [16] was used to calculate the quantity of *ShCuZnSOD* and *ShMnSOD* mRNA relative to 40S ribosomal protein S7 mRNA and the quantity of RfCuZnSOD and RfMnSOD mRNA relative to *RfEF1α*. Relative *ShCuZnSOD, ShMnSOD, RfCuZnSOD* and *RfMnSOD* mRNA levels for each tissue were calculated by comparison with mRNA expression levels in skin, pouch, and gill respectively. Post-infection temporal expression was compared with the PBS control at each corresponding time point to determine expression-fold changes after challenge.

2.11 Statistical analysis

All the assays were performed in triplicate and the data are reported as means ± SD. Statistically significant differences were identified with unpaired, two-tailed t-test to calculate P-values using GraphPad (GraphPad Software, Inc., USA).

Table 1. Description of primers

Primer Name	**Primer Sequence**
ShCuZnSOD-F_cloning	GAGAGAgaattcATGGCGCTTAAAGCCGTTTGTG
ShCuZnSOD-R_cloning	GAGAGAaagcttTTACTGGGTGATGCCGATGACG
ShMnSOD-F_cloning	GAGAGAgatatcATGCTCTGCAGAGTTGCTCAGATCC
ShMnSOD-R_cloning	GAGAGAgaattcTTATTTCTTTGCAGTCTGGAGACGCTCG
RfCuZnSOD-F_cloning	GAGAGAgatatcATGGTGCTGAAAGCTGTCTGTGTG
RfCuZnSOD-R_cloning	GAGAGAgaattcTTACTGGGCGATGCCGATGAC
RfMnSOD-F_cloning	GAGAGAgatatcATGCTGTGCAGAGTCGGACAGATA
RfMnSOD-R_cloning	GAGAGAgaattcCTACTTTTTGGCTGTCTGGAGACGC
ShCuZnSOD-F_qPCR	CGAAACCAGCGGAACGGTGTATTT
ShCuZnSOD-R_qPCR	TTCTGGAGTGGGTTGAAGTGAGGT
ShMnSOD-F_qPCR	GCTACGACAAACAAGGCGGAAGAC
ShMnSOD-R_qPCR	TCTCCCAGTTGATGACGTTCCAGATG
RfCuZnSOD-F_qPCR	ATGATTCAGACCCGGTGAAGCTGA
RfCuZnSOD-R_qPCR	AGGTCTCCAACATGCCTATGCTCA
RfMnSOD-F_qPCR	AAGGGAGATGTGACAGCACAGGTT
RfMnSOD-R_qPCR	AGCCGCAGACATCTTCTCCTTCAT
Sh40S ribosomal protein-F_qPCR	GCGGGAAGCATGTGGTCTTCATT
Sh40S ribosomal protein-R_qPCR	ACTCCTGGGTCGCTTCTGCTTATT
RfEf1α-F_qPCR	AACCTGACCACTGAGGTGAAGTCTG
RfEf1α-R_qPCR	TCCTTGACGGACACGTTCTTGATGTT

F; forward, R; reverse

3. Chapter I

Identification and molecular characterization of ShCuZnSOD and RfCuZnSOD while deciphering their roles in host acute phase response.

3.1 *In silico* analysis of CuZnSODs

3.1.1 *Delineation of sequence features and domain architecture*

The complete coding sequence of ShCuZnSOD and RfCuZnSOD were identified by homology screening of the seahorse cDNA transcriptomic database and rockfish cDNA transcriptomic database respectively. ShCuZnSOD was comprised of 842 bp including a 5' untranslated region (UTR) of 67 bp, a CDS of 465 bp that encodes a peptide of 154 amino acids (aa) and a 3' UTR of 313 bp (Fig. 1A). RfCuZnSOD was comprised of 853 bp including 5' UTR of 121 bp, a CDS of 465 bp that encodes a peptide of 154 aa and a 3' UTR of 267 bp (Fig. 1B). Similarly, the corresponding polypeptides in other organisms are range from 154 to 155 aa. The ProtParam tool predicted that the encoded ShCuZnSOD protein had a molecular mass of 15.94 kDa and a theoretical pI value of 5.73 where RfCuZnSOD protein had molecular mass of 16.04 kDa with a theoretical pI value of 5.88. The predicted molecular masses of the ShCuZnSOD and RfCuZnSOD are also similar to those of other CuZnSODs [13, 17-19]. The high pI of those CuZnSODs is important for the copper binding activity of histidine in ShCuZnSOD and RfCuZnSOD [20]. However, Rubino et al. [21] demonstrated that lower pH (<4) leads to a reduction of copper binding affinity. Due to the high pI value of ShCuZnSOD and RfCuZnSOD, pH does not affect the reduction of the copper binding affinity [20]. Low instability indexes of 14.98 and 2.67 were predicted, suggesting that the ShCuZnSOD and RfCuZnSOD proteins were stable.

(A)

```
                                                              GTTGGCT -67
TGGCCCTGACTCGTT TGCATCGACGTCCGA ATCGCCGTGCAGCAA ACTATCTCGAACAAA -60
ATGGCGCTTAAAGCC GTTTGTGTGCTGAGA GGAACCGGCGAAACC AGCGGAACGGTGTAT  60
 M  A  L  K  A   V  C  V  L  R   G  T  G  E  T   S  G  T  V  Y   20
TTCCAGCAGGAGAGC GAGTCCAGCCCTGTG AAGCTGACGGGACAA ATCGATGGCCTCACG 120
 F  Q  Q  E  S   E  S  S  P  V   K  L  T  G  Q   I  D  G  L  T   40
CCAGGCGAGCACGGC TTCCACGTCCACACC TTTGGAGACAACACG AACGGGTGTATCAGT 180
 P  G  E  H  G   F  H  V  H  T   F  G  D  N  T   N  G  C  I  S   60
GCTGGACCTCACTTC AACCCACTCCAGAAA AATCACGCCGGTCCG AACGATCCAGACAGG 240
 A  G  P  H  F   N  P  L  Q  K   N  H  A  G  P   N  D  P  D  R   80
CATGTCGGCGACCTC GGCAACGTGACCGCG GGTGCCGATAAGGTG GCCAAACTCGACATC 300
 H  V  G  D  L   G  N  V  T  A   G  A  D  K  V   A  K  L  D  I  100
ACAGACAGTGTGATC TCCCTCACCGGCCCA AACTCAATTATTGGC AGAACCATGGTGATC 360
 T  D  S  V  I[  S  L  T  G  P   N  S  I  I  G   R  T  M  V  I  120
CACGAGAAGGCAGAT GACTTGGGGAAAGGC AACAACGAGGAGAGC TTAAAGACGGGTAAC 420
 H  E  K  A  D   D  L  G  K  G   N  N  E  E  S   L  K  T  G  N  140
GCCGGCGGACGTCTG GCTTGCGGCGTCATC GGCATCACCCAGTAA AAAACACCACTGCGA 480
 A  G  G  R  L   A  C  G  V  I   G  I  T  Q  *                  154
AACCATGGAAGCTTA ATGCACTTAAAAAGA CCAACTGAGCTACTG GGTGTGATTGTGTTT 540
TTGTTTTTGTTTTTT TGACCATTTAATGAG CCTACATCCATGCTA TTGTATGCTTGGACC 600
CCAAAAGATGTTGTG CACATGTTGTAAACT GACAGACAACAAAGA TTAAATAAAGAGTTC 660
ATCTTCAAAAAAAAA AAAAAAAAACAAAAA AAAAAAAAAAAAAAA AAAAAAAAAAAAAAA 720
AAAAAAAAAAAAAAA AATAAAAAAAAAAAA ATAAAAAAAAAAAAA GAAAAAAAAA      775
```

(B)

```
                                                                C -121
CAGGTCTCCAACATG CCTATGCTCATCAGT AGGACCGGCATGATC CTTGCCGTGGGGATT -120
GAAGTGAGGGCCTGC ACTGATGCCAAGAGC GACACAAACTTGAAC GTCCTGACTGCAAAG  -60
ATGGTGCTGAAAGCT GTCTGTGTGTTGAAA GGAGCCGGAGACACC ACCGGGACCGTGTTT   60
 M  V  L  K  A   V  C  V  L  K   G  A  G  D  T   T  G  T  V  F    20
TTTGAGCAGGAGAAT GATTCAGACCCGGTG AAGCTGACAGGAGAA ATCAAAGGCCTTACT  120
 F  E  Q  E  N   D  S  D  P  V   K  L  T  G  E   I  K  G  L  T    40
CCCGGTGAGCATGGT TTCCATGTCCATGCT TTTGGAGACAATACG AACGGGTGCATCAGT  180
 P  G  E  H  G   F  H  V  H  A   F  G  D  N  T   N  G  C  I  S    60
GCAGGCCCTCACTTC AATCCCCACGGCAAG GATCATGCCGGTCCT ACTGATGAGCATAGG  240
 A  G  P  H  F   N  P  H  G  K   D  H  A  G  P   T  D  E  H  R    80
CATGTTGGAGACCTG GGGAATGTGACTGCA AATGCAGAAAATGTT GCCAAGCTAGACTTC  300
 H  V  G  D  L   G  N  V  T  A   N  A  E  N  V   A  K  L  D  F   100
ACGGACAAAGTAATC ACCCTTGCTGGCCCG CACTCCATCATTGGC AGAACTATGGTGATC  360
 T  D  K  V  I   T  L  A  G  P   H  S  I  I  G   R  T  M  V  I   120
CACGAGAAGAAAGAC GACCTGGGAAAAGGA GGCAATGAGGAGAGT CTAAAGACGGGCAAT  420
 H  E  K  K  D   D  L  G  K  G   G  N  E  E  S   L  K  T  G  N   140
GCTGGTGCACGTCTG GCCTGCGGTGTCATC GGCATCGCCCAGTAA ACTCTGCTAGAACTT  480
 A  G  A  R  L   A  C  G  V  I   G  I  A  Q  *                   154
GCAGCACTGGAAACA ACTTTCCCCCAAAGC ATTTAATAAGACCAA CATAGCTACTTAATG  540
TGACGTTTGTCCTTT TCAATACTCTGTGGC ATTTTATTGACTAGT CTAGAGAGTAGTTGA  600
GCCATGCTTTTACGT GGTCTGTTCCTCATA ACAGTTGTATGTATG GATTTATATGTCTGC  660
TGATTTAGTTTTGGT CCCAAAGAATTGGTA ACGCACAAGTAATAA ACAGATGTACACAAG  720
TTCTCAGTTAAT
```

Figure 1. Domain architecture of (A) ShCuZnSOD and (B) RfCuZnSOD. "✩" correspond to the active sites. The Cu^{2+} binding sites are denoted by bold, italicized blue letters. Zn^{2+} binding sites are underlined in black. Polypeptide binding sites are round in black. *N*-glycosylation sites are denoted by a green rectangular. Copper/Zinc superoxide dismutase signature 1 is denoted by a black rectangular and Copper/Zinc superoxide dismutase signature 2 is denoted by a red rectangular.

Analysis of the protein sequences indicated that both ShCuZnSOD and RfCuZnSOD did not contain signal peptide or transmembrane regions. These CuZnSODs are located within the cytoplasm. Immunolocalization studies have shown that CuZnSODs are present in the major organelles where ROS are generated, including the cytoplasmic matrix, nucleus, and mitochondrial interspace membrane, affirming their role in redox balance [22]. A putative *N*-glycosylation site (^{87}NVTA^{90}) was present, as a typical Cu/Zn_SOD domain at 3-147 aa in ShCuZnSOD sequence. Contrarily, two *N*-glycosylation sites were observed in the RfCuZnSOD sequence at N^{25} and N^{87}. These putative *N*-glycosylation sites identified in ShCuZnSOD and RfCuZnSOD indicate that they might be glycoproteins [13, 23]. PROSITE results revealed two signature motifs and three cysteine residues in both ShCuZnSOD and RfCuZnSOD. These cysteine residues were predicted to form an intra-chain disulfide bond. CuZnSODs can form a homodimer in which the two subunits are stabilized by an intra-subunit disulfide bond [24]. The conserved cysteine residues have been suggested to contribute to structural integrity and biological function by stabilizing CuZnSODs under high temperature conditions [25, 26]. The *in silico* analysis identified four Cu^{2+} binding sites and four Zn^{2+} binding sites within the Cu/Zn_SOD domain in both CuZnSODs. Moreover, conserved active residues, including the histidines and the aspartic acid, support the presumed functional similarity to other orthologs. Among these conserved sequences, there are several electro-statistically relevant residues known to contribute to the recognition of superoxide anion substrates [27]. The MultiLoc tool showed that ShCuZnSOD and RfCuZnSOD were likely located in the cytoplasm (accuracy of 0.98).

3.1.2 *Homology analysis*

The ClustalW pairwise comparison showed that the highest amino acid identity of ShCuZnSOD was with *Siniperca chuatsi* (87.7%) followed by *Maylandia zebra* and *Oplegnathus fasciatus* (85.7%). In addition, the similarities of these proteins were 92.9% (Fig. 2A). Regarding with the RfCuZnSOD the highest amino acid identity was showed with the *Lates calcarifer* (87 %) followed by *Oplegnathus fasciatus* (86.4%). There similarities were as 92.9 % and 90.9% respectively (Fig. 2B). The degree of conservation and homology of CuZnSODs among different taxa suggests the structural importance of these proteins as antioxidants.

(A)

ShCuZnSOD			*H. abdominalis*	*O. fasciatus*	*T. obscurus*	*S. aurata*	*A. japonica*	*O. mykiss*	*H. molitrix*	*S. salar*	*D. rerio*	*C. idella*	*O. latipes*	*M. musculus*	*H. discus discus*	*X. laevis*	*S. scrofa*	*R. norvegicus*	*B. taurus*	*G. gallus*
Scientific Name	**Accesion No**		Identity%																	
Hippocampus abdominalis	KU665493	Similarity%		85.7	83.8	81.2	79.9	78.6	77.3	77.3	76.6	76	74.7	70.1	69.5	68.8	68.8	68.2	67.5	66
Oplegnathus fasciatus	AAT36615		92.9		90.3	89.6	85.1	85.7	81.8	82.5	81.2	81.8	82.5	70.8	69.5	68.2	70.1	68.8	68.2	64.1
Takifugu obscurus	ABV24054		92.2	96.8		86.4	84.4	83.8	79.9	80.5	81.2	79.9	75.3	69.5	66.9	67.5	68.8	67.5	66.2	63.5
Sparus aurata	AFV39806		89.0	92.9	92.2		83.1	83.1	83.8	79.9	81.8	83.8	84.4	72.1	68.2	70.1	68.8	71.4	68.8	65.4
Anguilla japonica	BAJ79017		88.3	89.6	90.9	87.7		83.1	77.3	81.2	80.5	77.9	77.9	72.1	70.1	70.1	70.1	71.4	70.1	65.4
Oncorhynchus mykiss	NP_001154086		87.0	90.9	90.3	87.0	90.9		78.6	86.4	81.8	79.2	74.0	68.2	71.4	68.2	67.5	66.2	64.9	62.2
Hypophthalmichthys molitrix	ADJ67808		87.7	90.3	87.7	89.6	87.7	86.4		76.6	85.7	96.8	77.3	74.7	69.5	68.2	70.8	72.1	72.7	63.5
Salmo salar	ACM08323		86.4	87.0	89.6	85.1	88.3	90.3	87.7		81.2	76.0	73.4	72.1	67.5	67.5	68.2	70.1	68.8	64.7
Danio rerio	NP_571369		85.1	87.7	89.6	85.1	88.3	88.3	89.6	88.3		86.4	74.0	71.4	73.4	66.9	70.8	70.1	70.1	66.0
Ctenopharyngodon idella	ADF31307		85.7	89.6	87.7	89.0	87.7	87.0	96.8	86.4	90.3		76.0	73.4	69.5	68.2	70.8	71.4	72.1	62.0
Oryzias latipes	XP_004076261		88.3	90.9	89.6	94.2	88.3	85.7	89.0	85.1	83.8	87.0		68.8	67.5	71.4	66.9	68.8	68.8	64.1
Mus musculus	NP_035564		79.9	81.2	81.8	81.2	83.8	80.5	85.1	81.8	81.8	83.8	81.8		68.8	65.6	83.1	96.8	84.4	71.2
Haliotis discus discus	ABG88844		77.3	76.6	79.2	76.0	81.8	79.9	78.6	76.0	80.5	78.6	76.0	79.9		66.9	66.9	67.5	71.0	66.0
Xenopus laevis	AAH70696		80.5	79.9	79.9	81.2	77.9	76.6	79.9	76.6	79.9	80.5	81.2	76.0	73.4		64.9	65.6	66.0	67.5
Sus scrofa	XP_005657198		78.6	78.6	79.9	76.6	80.5	76.6	77.9	77.3	76.0	77.9	77.3	89.0	76.6	75.3		81.8	84.4	72.4
Rattus norvegicus	NP_058746		78.6	79.9	80.5	81.2	82.5	79.2	83.8	80.5	80.5	83.1	81.8	98.7	78.6	76.0	88.3		83.1	71.2
Bos taurus	NP_777040		77.3	77.9	79.2	77.9	79.9	76.6	81.2	78.6	79.9	81.2	78.6	90.3	81.2	74.3	91.6	89.6		72.9
Gallus gallus	NP_990395		78.6	78.6	80.5	79.2	79.9	76.0	79.2	77.9	78.6	78.6	79.2	83.8	79.2	79.2	83.1	84.4	82.5	

(B)

RfCuZnSOD			*S. schlegelii*	*L. calcarifer*	*O. fasciatus*	*S. aurata*	*E. coioides*	*M. zebra*	*T. obscurus*	*H. abdominalis*	*O. mykiss*	*S. salar*	*D. rerio*	*M. musculus*	*R. norvegicus*	*B. taurus*	*S. scrofa*	*H. discus discus*	*X. laevis*	*G. gallus*	*G. hirsutum*	*A. baumannii*
Scientific name	**Accession No**		Identity%																			
Sebastes schlegelii		Similarity%		87	86.4	85.7	85.1	84.4	83.8	79.9	79.9	79.9	78.6	70.8	68.8	68.2	67.5	67.5	66.2	64.7	48.8	31.1
Lates calcarifer	ADT82684		92.9		93.5	89.0	90.9	90.3	89.6	85.1	83.1	79.9	79.2	71.4	69.5	69.5	70.1	67.5	68.8	65.4	49.4	30.5
Oplegnathus fasciatus	AAT36615		90.9	96.1		89.6	90.3	92.2	90.3	85.7	85.7	82.5	81.2	70.8	68.8	68.2	70.1	69.5	68.2	64.1	50.0	29.9
Sparus aurata	AFV39806		91.6	93.5	92.9		89.0	86.4	86.4	81.2	83.1	79.9	81.8	72.1	71.4	68.8	68.8	68.2	70.1	65.4	50.0	29.8
Epinephelus coioides	AAW29025		92.2	95.5	94.2	93.5		86.4	90.3	82.5	81.2	80.5	79.2	68.8	66.9	68.2	68.2	65.6	68.2	66.0	46.9	31.7
Maylandia zebra	XP_004550117		89.6	94.8	96.1	92.9	92.9		87.0	85.7	83.1	79.2	77.9	70.8	68.8	68.8	70.1	70.8	68.8	64.1	48.8	28.1
Takifugu obscurus	ABV24054		90.9	94.8	96.8	92.2	95.5	93.5		83.8	83.8	80.5	81.2	69.5	67.5	66.2	68.8	66.9	67.5	63.5	46.9	29.9
Hippocampus abdominalis	KU665493		87.7	90.9	92.9	89.0	89.6	92.9	92.2		78.6	77.3	76.6	70.1	68.2	67.5	68.8	69.5	68.8	66.0	48.1	29.3
Oncorynchus mykiss	NP_001154086		85.7	90.3	90.9	87.0	87.7	89.6	90.3	87.0		86.4	81.8	68.2	66.2	64.9	67.5	71.4	68.2	62.2	50.0	29.9
Salmo salar	ACM08323		87.0	87.7	87.0	85.1	87.7	85.7	89.6	86.4	90.3		81.2	72.1	70.1	68.8	68.2	67.5	67.5	64.7	48.8	31.7
Danio rerio	NP_571369		86.4	87.7	87.7	85.1	86.4	86.4	89.6	85.1	88.3	88.3		71.4	70.1	70.1	70.8	73.4	66.9	66.0	51.2	31.7
Mus musculus	NP_035564		81.2	81.8	81.2	81.2	83.1	79.9	81.8	79.9	80.5	81.8	81.8		96.8	84.4	83.1	68.8	65.6	71.2	55.6	28.0
Rattus norvegicus	NP_058746		79.9	80.5	79.9	81.2	81.8	78.6	80.5	78.6	79.2	80.5	80.5	98.7		83.1	81.8	67.5	65.6	71.2	54.9	27.4
Bos taurus	NP_777040		77.9	79.9	77.9	77.9	79.9	77.3	79.2	77.3	76.6	78.6	79.9	90.3	89.6		84.4	71.0	66.0	72.9	54.0	30.7
Sus scrofa	XP_005657198		76.0	77.9	78.6	76.6	78.6	77.3	79.9	78.6	76.6	77.3	76.0	89.0	88.3	91.6		66.9	64.9	72.4	54.3	29.2
Haliotis discus discus	ABG88844		76.6	75.3	76.6	76.0	75.3	78.6	79.2	77.3	79.9	76.0	80.5	79.9	78.6	81.2	76.6		66.9	66.0	51.2	32.1
Xenopus laevis	AAH70696		76.6	79.9	79.9	81.2	79.9	80.5	79.9	80.5	76.6	76.6	79.9	76.0	76.0	74.3	75.3	73.4		67.5	52.2	31.7
Gallus gallus	NP_990395		76.0	80.5	78.6	79.2	80.5	77.9	80.5	78.6	76.0	77.9	78.6	83.8	84.4	82.5	83.1	79.2	79.2		55.3	33.3
Gossypium hirsutum	ACC93639		63.4	65.2	64.6	63.4	64.6	65.2	65.2	64.6	65.2	64.6	64.6	67.7	67.7	66.5	65.8	65.2	64.0	65.8		27.6
Acinetobacter baumannii	WP_011860386		48.1	46.8	46.8	48.1	47.4	44.2	46.8	46.1	44.8	48.7	50.6	48.1	46.8	49.4	48.7	48.1	48.1	48.7	42.9	

Figure 2. Identity and similarity of (A) ShCuZnSOD and (B) RfCuZnSOD to other vertebrate and invertebrate counterparts.

The results of the multiple sequence alignment revealed that both ShCuZnSOD (Fig. 3A) and RfCuZnSOD (Fig. 3B) shared a common consensus pattern with its homologs. The Cu^{2+} binding sites and the Zn^{2+} binding sites were strongly conserved among the selected species. The *N*-glycolic residue was also highly conserved, while the residues in the two Cu/Zn signatures were largely conserved. The two cysteine residues (Cys^{58} and Cys^{158}) required for disulfide bridge formation were conserved (Fig. 3). CuZnSODs can form a homodimer in which the two subunits are stabilized by an intra-subunit disulfide bond [24].

(A)

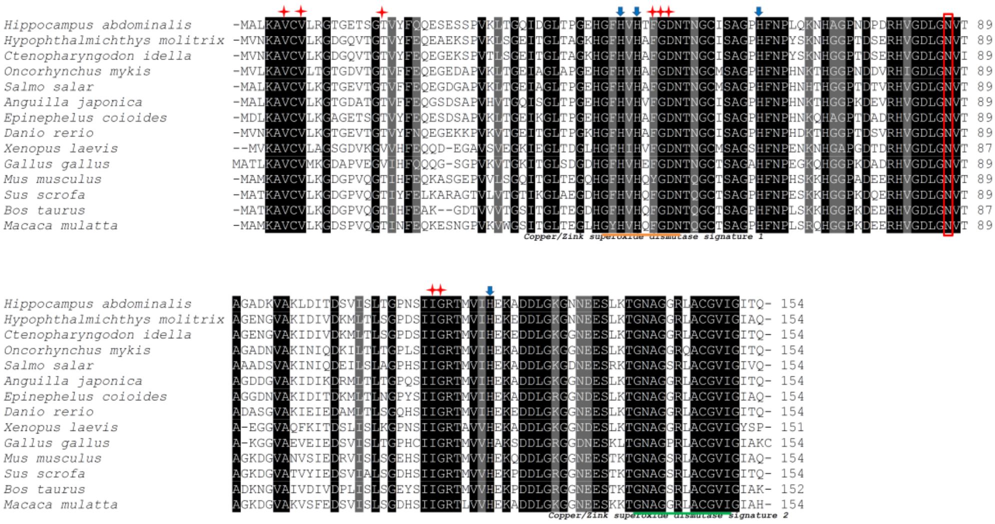

(B)

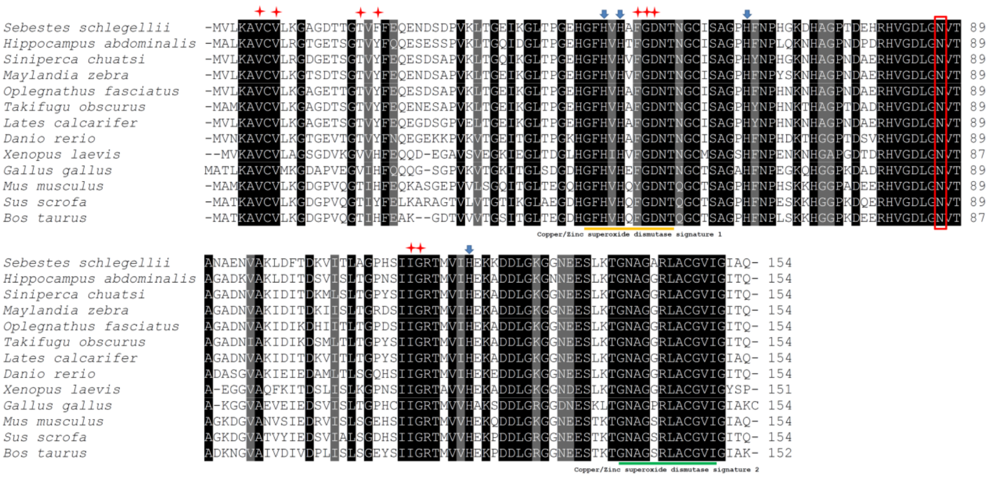

Figure 3. Multiple sequence alignment of (A) ShCuZnSOD and (B) RfCuZnSOD with vertebrate and invertebrate counterparts. Residues that are highly conserved are shaded in black and similarities among the orthologs are gray shaded. *N*-glycosylation site is in a red box. Red stars denote the active sites and the blue arrows denote the Cu^{2+} binding sites.

3.1.3 *Phylogenetic reconstruction*

A phylogenetic tree was generated to analyze the evolutionary relationship of ShCuZnSOD and RfCuZnSOD; the tree was constructed by the NJ method using the amino acid sequences of selected orthologs. ShCuZnSOD fell into the same clade as a group of fish counterparts and was separate from other vertebrate and plant counterparts (out-group). ShCuZnSOD was evolutionarily close to *M. zebra* CuZnSOD (Fig. 4A). Likewise, RfCuZnSOD also clade with the fish counterparts affirming RfCuZnSOD belongs to the fish group (Fig. 4B). The closest relationship of RfCuZnSOD is with *L. calcarifer*. Generally, the CuZnSOD seemed to be evolved at a constant rate while distinct from other SODs and it was noted that CuZnSOD is rapidly evolved during the recent years but slower at the beginning [28, 29].

Overall, the results from pairwise alignments and phylogenetic analysis showed ShCuZnSOD and RfCuZnSOD had a close relationship with other fish homologs and indicated that it belonged to the fish SOD family. The conserved sequence architecture and motifs of CuZnSODs suggest that they share similar functions in a wide range of organisms [30, 31].

(A)

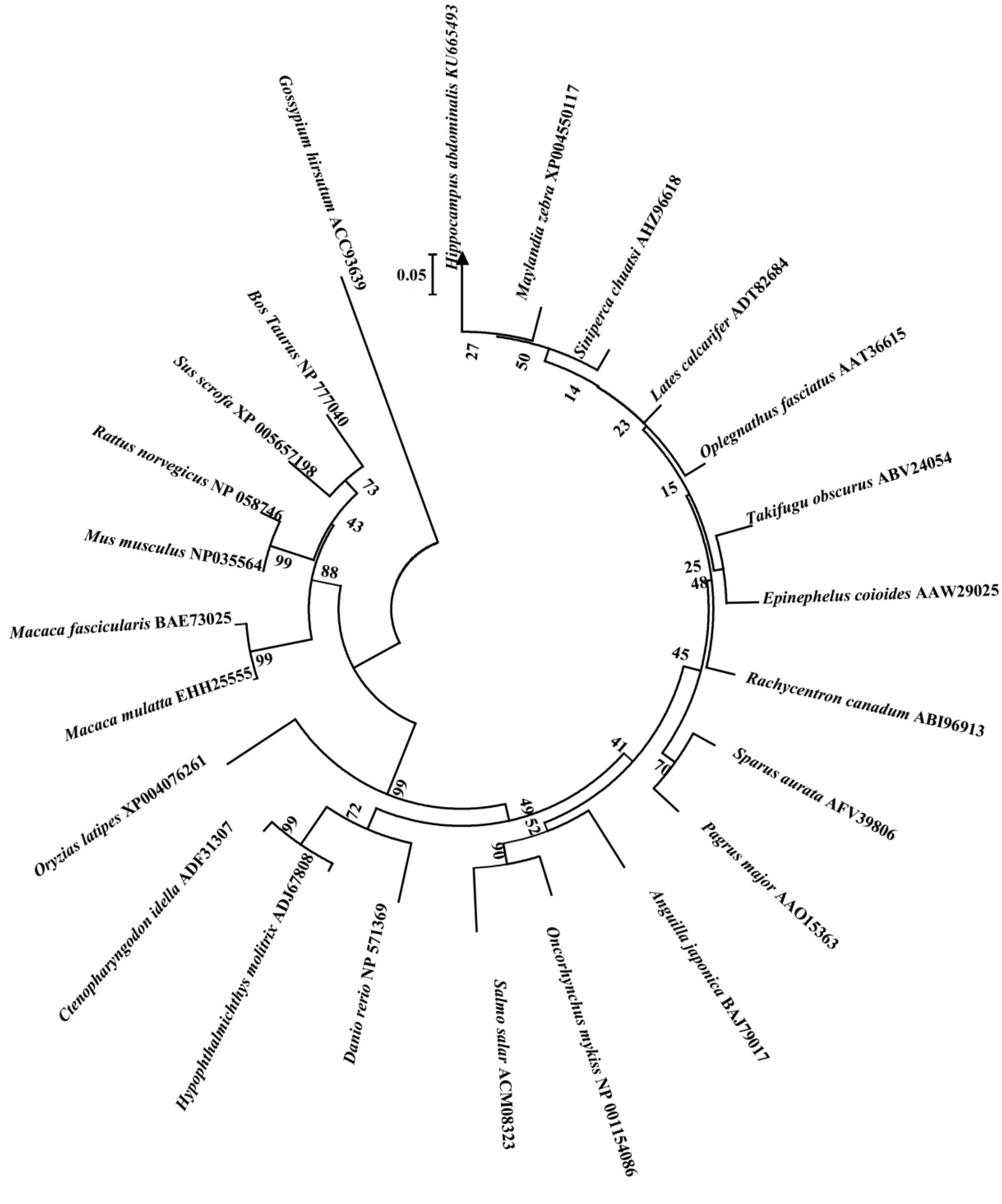
Hippocampus abdominalis KU665493
Maylandia zebra XP004550117
Siniperca chuatsi AHZ96618
Lates calcarifer ADT82684
Oplegnathus fasciatus AAT36615
Takifugu obscurus ABV24054
Epinephelus coioides AAW29025
Rachycentron canadum ABI96913
Sparus aurata AFV39806
Pagrus major AAO15363
Anguilla japonica BAJ79017
Oncorhynchus mykiss NP 001154086
Salmo salar ACM08323
Danio rerio NP 571369
Hypophthalmichthys molitrix ADJ67808
Ctenopharyngodon idella ADF31307
Oryzias latipes XP004076261
Macaca mulatta EHH25555
Macaca fascicularis BAE73025
Mus musculus NP035564
Rattus norvegicus NP 058746
Sus scrofa XP 005657198
Bos Taurus NP 777040
Gossypium hirsutum ACC93639
0.05

(B)

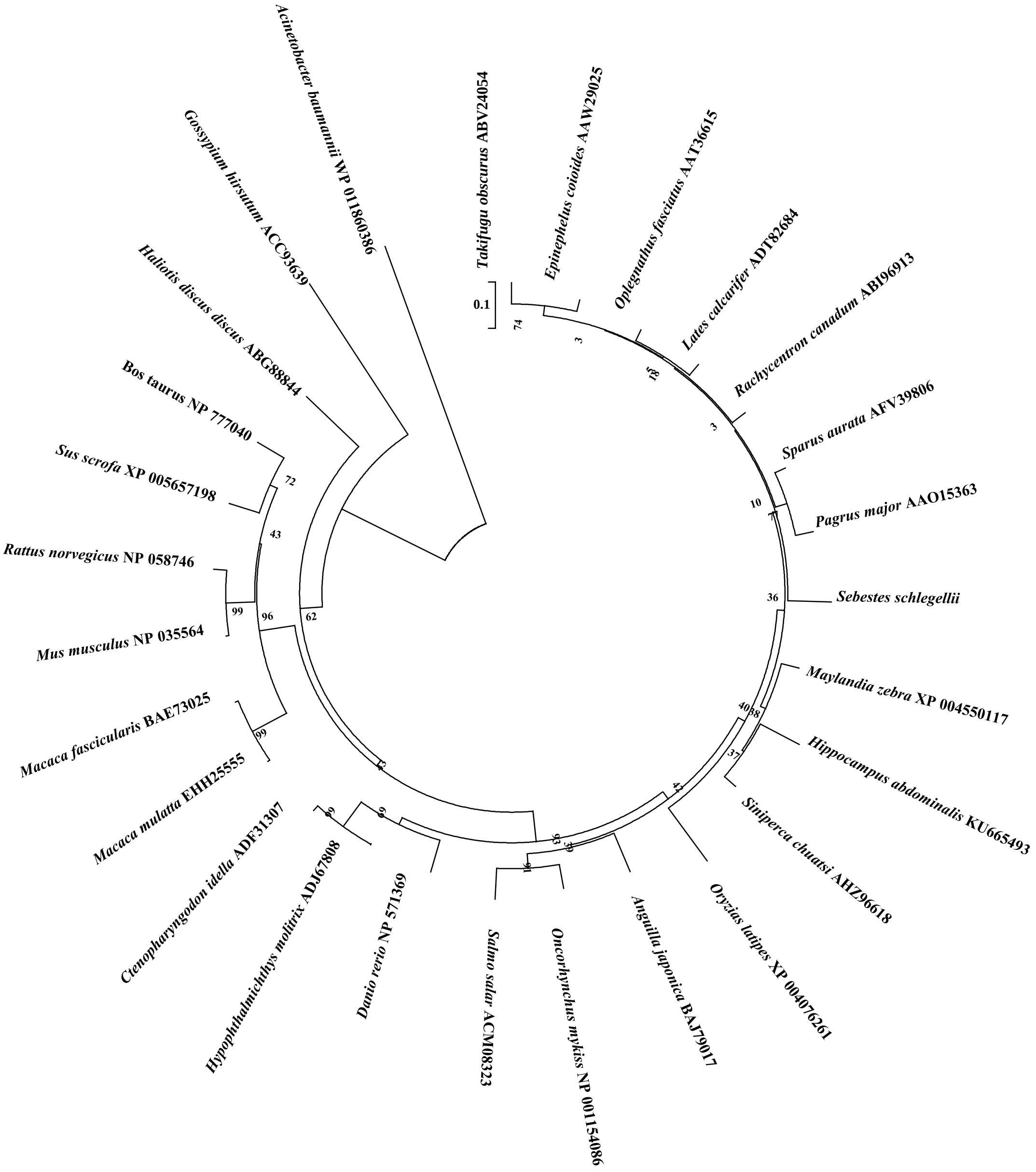

Figure 4. Unrooted phylogenetic tree depicting the relationship of (A) ShCuZnSOD, (B) RfCuZnSOD and its known orthologs. Numbers at the nodes indicate percent bootstrap confidence values derived from 5000 replications.

3.1.4 *Tertiary structural characterization*

The structure of the ShCuZnSOD and the RfCuZnSOD homodimers were determined by using the template of a mouse-human CuZnSOD chimera (TMscore, 0.92 ± 0.06; RMSD, 2.0 ± 1.6 Å). Both three-dimensional structures had a β-sheet barrel with 8 β-sheets and two short α helical region (Fig. 5). The cysteine residues of these CuZnSOD homodimers (Fig. 5A) were crucial for the formation of disulfide bridges between the CuZnSOD monomers [32]. In addition, the Cu^{2+} (Fig. 5B) and Zn^{2+} binding sites (Fig. 5C) of CuZnSODs were located together to ensure the catalytic function.

(X)

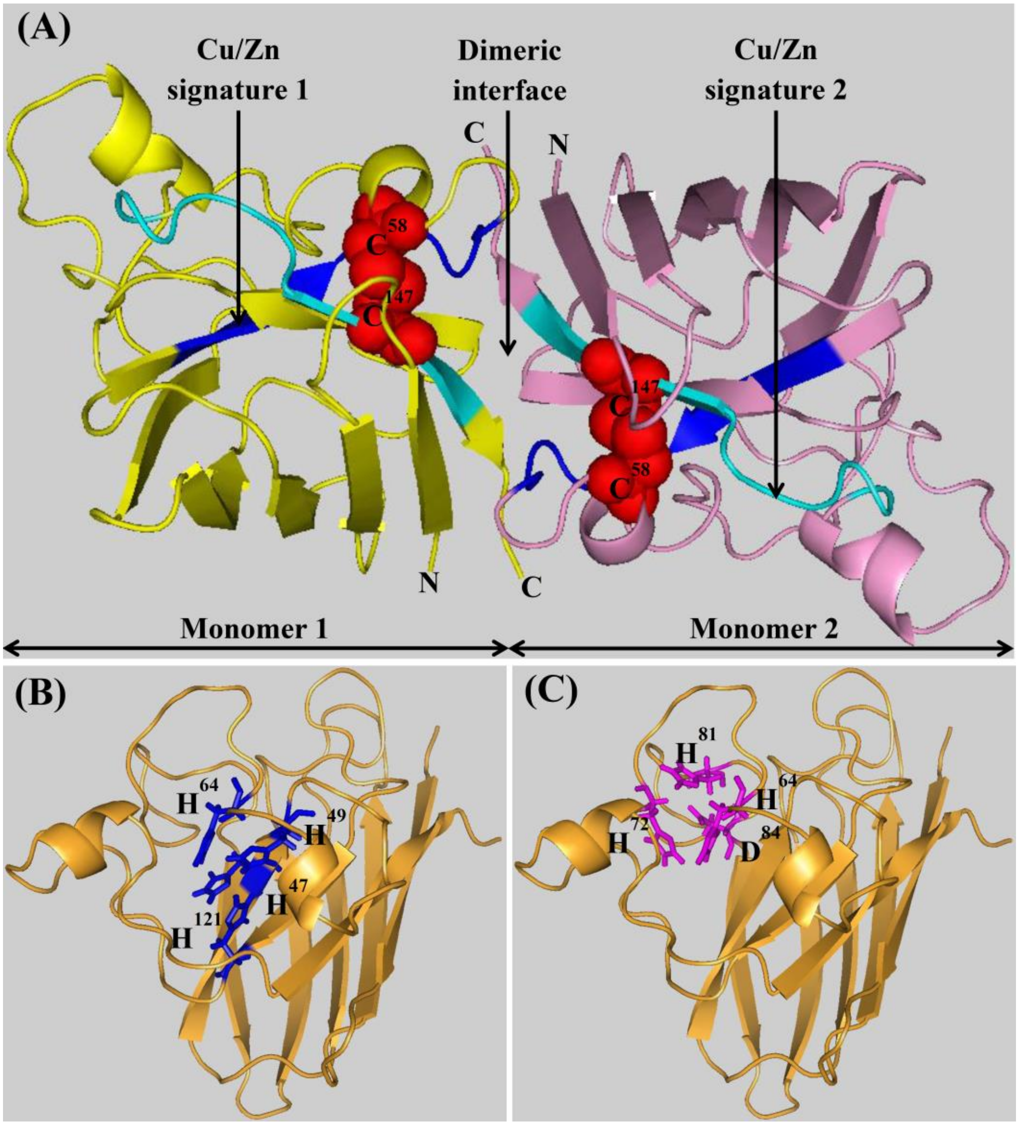

(Y)

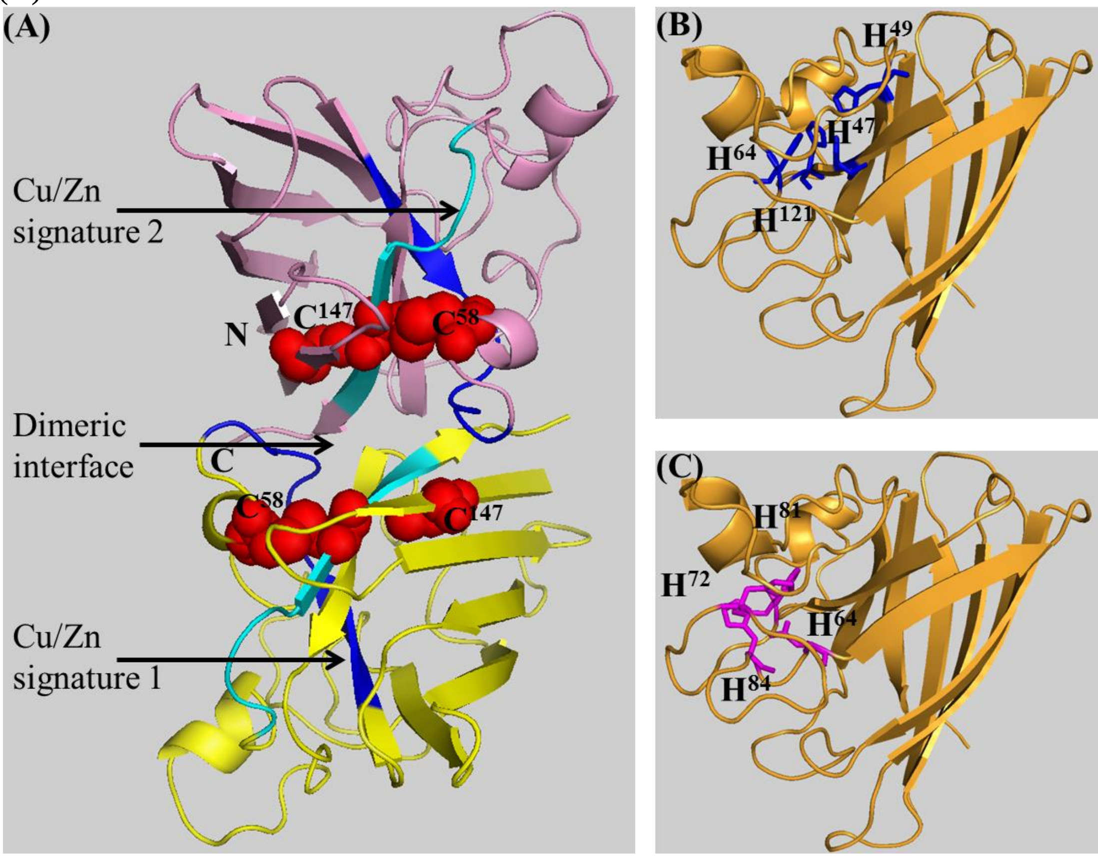

Figure 5. Predicted molecular model of the (X) ShCuZnSOD and (Y) RfCuZnSOD tertiary structure. (A) Homodimer of ShCuZnSOD. The interface between monomers is located at the C- and N-terminals, which are indicated by the respective letters. Cysteine residues are denoted by the red spheres. Cu/Zn signature 1 is demarcated in dark blue and Cu/Zn signature 2 in light blue. (B) Cu^{+2} binding sites, and (C) Zn^{+2} binding sites.

3.2 Antioxidant activity analysis of rCuZnSODs

3.2.1 *Protein expression and purification*

rShCuZnSOD and rRfCuZnSOD were successfully overexpressed in ER2523 (NEB Express) cells and purified. Reducing SDS-PAGE analysis of samples obtained at different phases of purification showed a strong and distinct band in the induced cell lysate. The purified rShCuZnSOD protein fused with MBP had a molecular mass of 58.44 kDa consistent with its estimated molecular weight and the purified rRfCuZnSOD protein fused with MBP had a molecular mass of 58.54 kDa.

3.2.2 *SOD assay with the effect of pH*

In order to determine the antioxidant function of ShCuZnSOD in the antioxidant system of the seahorse, the xanthine/XOD assay was performed. It is based on the ability of SOD to inhibit dye formation in the system. Xanthine is converted into uric acid and H_2O_2, while leaving $O_2\bullet^-$ radical as a byproduct. Those superoxide radicals convert the nitroblue tetrazolium (NBT) into NBT-diformazan dye, which allows the absorption of the light at a wave length of 560 nm. Reduction of the formation of the NBT-diformazan *via* dismutation of the superoxide radicals by SODs could be measured as the SOD activity.

(A) (B)

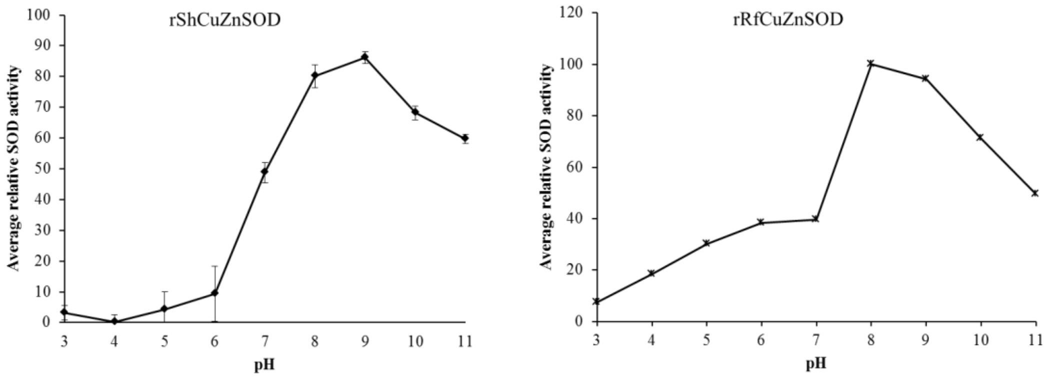

Figure 6.1 Xanthine/XO assay for the determination of optimum pH for (A) rShCuZnSOD and (B) rRfCuZnSOD.

The purified recombinant protein was used in a standard xanthine/XOD assay to investigate the antioxidant potential of two rCuZnSODs and to investigate the effects of pH and temperature on the activity. A range of pH 3 to pH 11 was used. The highest activity of rShCuZnSOD was observed at pH 9; below pH 5, no significant activity was found in the assay (Fig. 6.1A). Contritely, optimum pH for the rRfCuZnSOD was pH 8 (Fig. 6.1B).

3.2.3 *SOD assay with the effect of temperature*

The xanthine/XOD assay was then performed at the optimum pH but with different temperatures from 10 to 70 °C. The highest activity was recorded at 25 °C for both rCuZnSODs. However, both rCuZnSOD showed significant activity in a wide range of temperatures (Fig. 6.2). Antioxidant activity fell drastically at 60 °C in rShCuZnSOD (Fig. 6.2A). Though rRfCuZnSOD (Fig. 6.2B) also showed a significant activity in a wide range of temperatures, the significant activity was quiet lower compare to than that of to the rShCuZnSOD.

(A) (B)

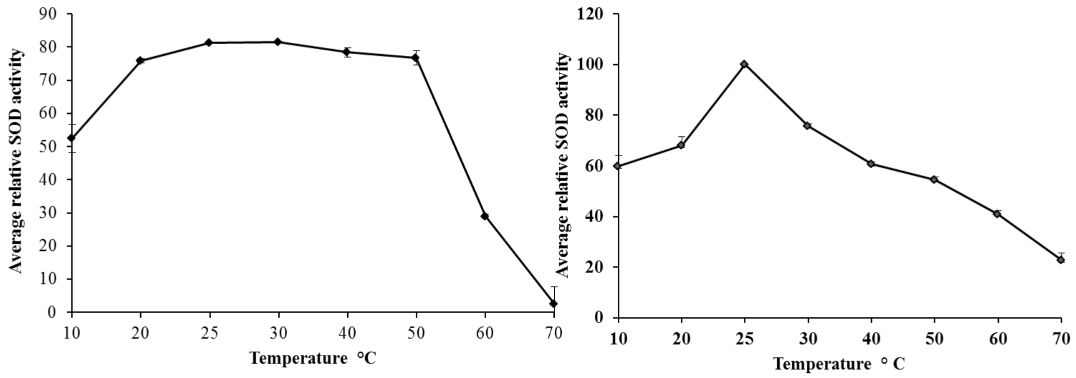

Figure 6.2 Xanthine/XO assay for the determination of optimum temperature for (A) rShCuZnSOD and (B) rRfCuZnSOD.

It is reported that SODs are found in a wide range of organisms and have higher stability in different pH and temperature conditions [33, 34]. Supporting to this statement SOD activity was observed in extreme pH and temperature conditions showing its stability to some extent. Also, the instability index of ShCuZnSOD is lower than 40 which is been referred as a stable protein [35]. The rShCuZnSOD showed higher activities at pH 9, thus it was more stable under alkaline conditions, and at 25 °C; where they could be the optimum conditions for the biological activity of seahorse SOD. Also the highest activity range was given around the pH 8-9 where it is more or less similar to the pH of their habitat, pH 8-8.3 [36]. Interestingly, previous studies have revealed that the alkaline pH is more favorable for the optimum function of the CuZnSOD because of its charged residues like lycine [37]. Also the electro static repulsion of $O_2^{\bullet-}$ radicals and the other negatively charged radicals cause the reduction of the dismutation process of the enzyme [38].

3.2.4 *Dose dependent antioxidant activity*

Antioxidant activity and average relative antioxidant activity were examined at different concentrations of the recombinant protein. According to the results the SOD activity was increased with the increasing concentration of both rCuZnSODs. rMBP did not have a significant impact on antioxidant activity (Fig. 6.3). Therefore, significant activity of the rCuZnSODs than that of rMBP reveals that rMBP is only an inert fusion companion, which had no influence on the antioxidant function of the rCuZnSODs.

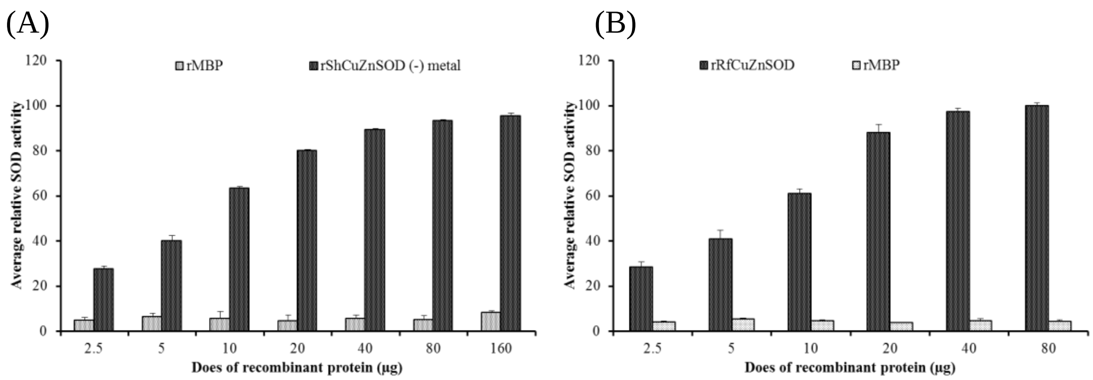

Figure 6.3 Xanthine/XO assay for the determination of dose dependent antioxidant activity (A) rShCuZnSOD and (B) rRfCuZnSOD.

3.2.5 *Effect of inhibitors*

The effect of inhibitors on the activity of two rCuZnSODs was analyzed using various candidate inhibitors, including KCN, DDC, NaN_3, and EDTA (Fig. 6.4). KCN, DDC, and NaN_3 showed significant effects on the relative activity of both rCuZnSODs but EDTA had no effect. However, KCN, DDC, and NaN3, inhibited antioxidant activity to different extents. Incidentally, stability of rCuZnSODs was highly demonstrated through the results of above different XOD assays which were more or less similar to the previous studies [33, 39, 40].

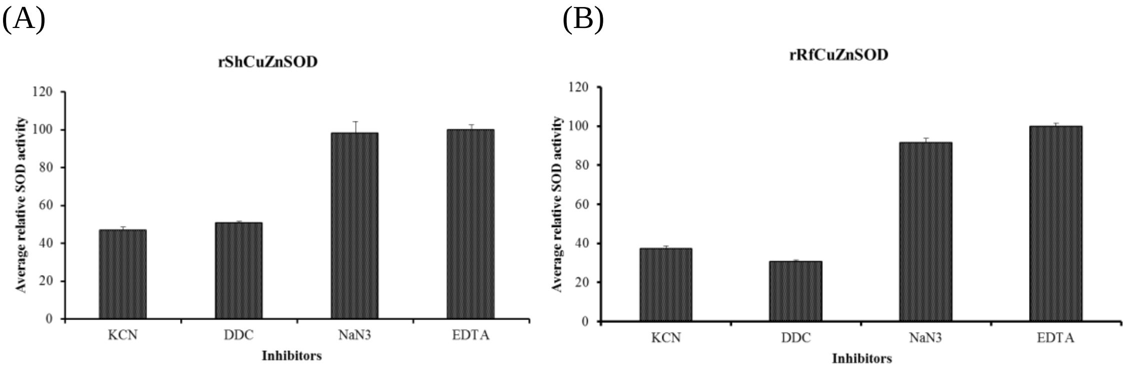

Figure 6.4 Effect of inhibitors on the antioxidant activity of (A) rShCuZnSOD and (B) rRfCuZnSOD.

3.3 Peroxidation function of rCuZnSOD

3.3.1 *Effect on cell viability*

The peroxidation function of both rShCuZnSOD and rRfCuZnSOD were assessed by investigating cell viability using an MTT assay of THP-1 cells under cytotoxic conditions after H_2O_2 treatment (Fig. 7). Cell viability increased in the presence of HCO_3^- and rCuZnSODs in a dose dependent manner; the highest percentages were observed in the 100 μg/mL of rCuZnSODs, which resulted in ~73% increase in rShCuZnSOD (Fig. 7A) and ~ 68% in rRfCuZnSOD (Fig. 7B). rMBP had no significant effect on cell viability.

(A) (B)

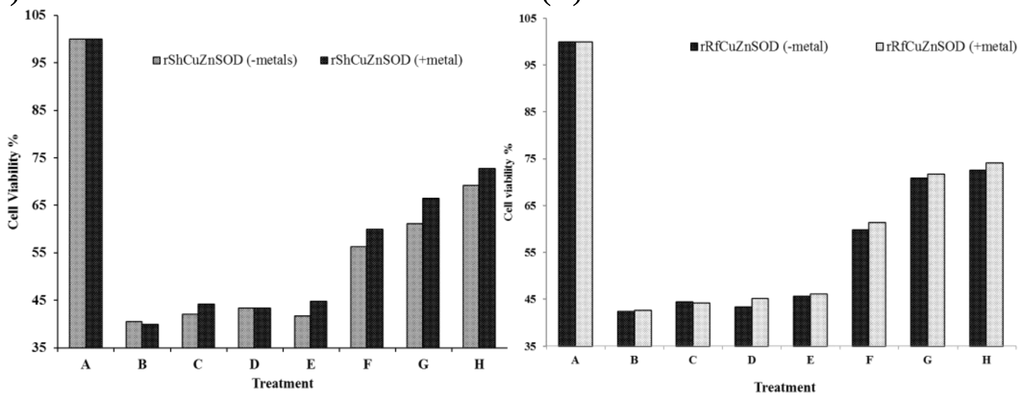

Figure 7. Relative cell viability in the presence of (A) rShCuZnSOD and (B) rRfCuZnSOD upon oxidative stress. An MTT assay was used to determine the rate of cell survival (%). Vertical bars represent cell viability % ± SD (N = 3). The treatments were as follows: (A) control cells, (B) 500 µmol H_2O_2, (C) 20 mM $NaHCO_3^-$ 500 µmol H_2O_2, (D) 100 µg/mL of MBP + 20 mM $NaHCO_3^-$ + 500 µmol of H_2O_2, (E) 25 µg/mL of rCuZnSOD + 20 mM $NaHCO_3^-$ + 500 µmol of H_2O_2, (F) 50 µg/mL of rCuZnSOD + 20 mM $NaHCO_3^-$ + 500 µmol of H_2O_2, (G) 75 µg/mL of rCuZnSOD + 20 mM $NaHCO_3^-$ + 500 µmol of H_2O_2 and (H) 100 µg/mL of rCuZnSOD + 20 mM $NaHCO_3^-$ + 500 µmol of H_2O_2.

Cell survival assay can be used to determine the ability of an enzyme or a protein to facilitate the viability of the cells against any oxidative stress. Generally, SODs are known to catalyze the superoxide radicals into oxygen and H_2O_2 [41]. Also it is known that H_2O_2 reacts with CuZnSOD which may leads to the disruption of its enzymatic activity [42]. However, it has been found that the decomposition of the H_2O_2 can be accomplished by the CuZnSOD in the presence of HCO_3^- or a structurally similar anion at physiological pH [43]. The role of the HCO_3^- in this system stands as it competes with other anions and binds to the anion-binding site of the CuZnSOD and that may assist the access of the H_2O_2 to the active site, empowering its redox breakage [43]. Therefore, here we have used HCO_3^- to facilitate the peroxidase activity of two rCuZnSODs. Based on this theory, effect of the rCuZnSODs on the cell viability against H_2O_2 oxidative stress was determined. According to the results, it was revealed that both rCuZnSOD have the cell protection activity against the H_2O_2-mediated oxidative stress by reducing the motility of the THP-1 cells. Specifically, the rCuZnSODs were acted as peroxidases and combat with the external H_2O_2 while minimizing the external oxidative stresses to the cells. Thereby, generation of intracellular ROSs in THP-1 cells compared to the absence of recombinant protein is very low. Hence, cell survival rate is significantly increased due to the potential peroxidation function of rCuZnSODs as detected in peroxiredoxin [44]. Meanwhile, the dose dependency of the rCuZnSODs proves that increasing concentration proportionally increases the cell viability while reducing the level of external H_2O_2.

Besides the comparison between metal supplemented and non-supplemented rCuZnSOD samples, the activities were quite higher in the metal supplemented samples. Therefore, binding of the sufficient metal ions to the rCuZnSOD could enhance its biological activity [39], as reported in rock bream rCuZnSOD [13]. Likewise, it has been reported that Zn has the ability to protect the cells from oxidative stress, while incorporate with other proteins or antioxidant enzymes with its antioxidant properties [45, 46].

3.3.2 *Extracellular ROS scavenging ability*

Extracellular H_2O_2 scavenging activity of rShCuZnSOD and rRfCuZnSOD in the presence of HCO_3^-, and the level of intracellular H_2O_2 in THP-1 cells were measured by flow cytometry (Fig. 8). Intracellular ROS levels in the cells fell drastically after 100 μg/mL of rCuZnSOD although the cells were exposed to oxidative stress by H_2O_2. Conversely, at 25 μg/mL rCuZnSODs, a relatively low reduction of intracellular ROS was observed compared to 100 μg/mL of rCuZnSOD. This effect was probably due to a low extracellular H_2O_2 scavenging activity at the low rCuZnSOD concentration. Contrarily, rMBP had no significant effect on extracellular H_2O_2 scavenging activity.

(A)

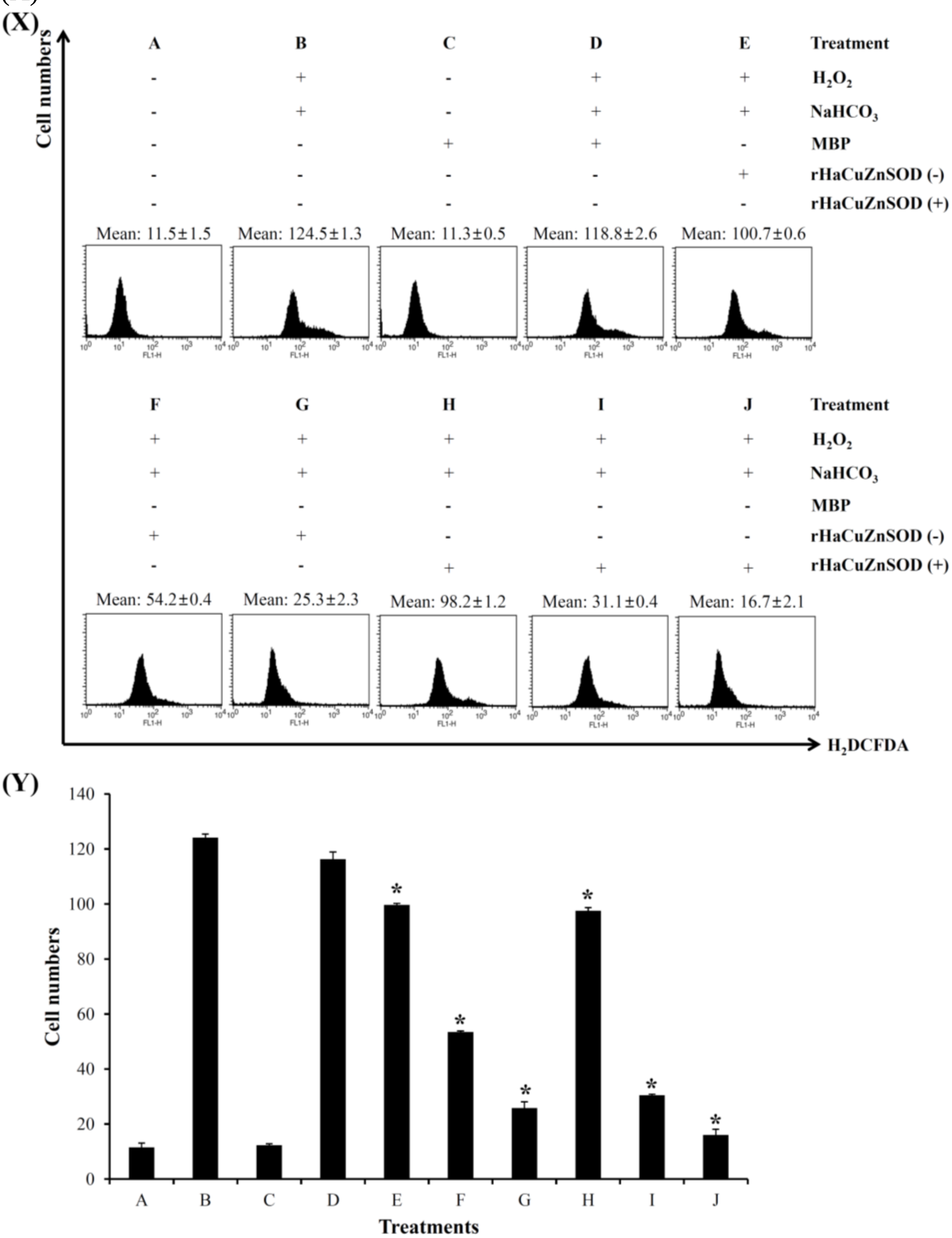

(B)

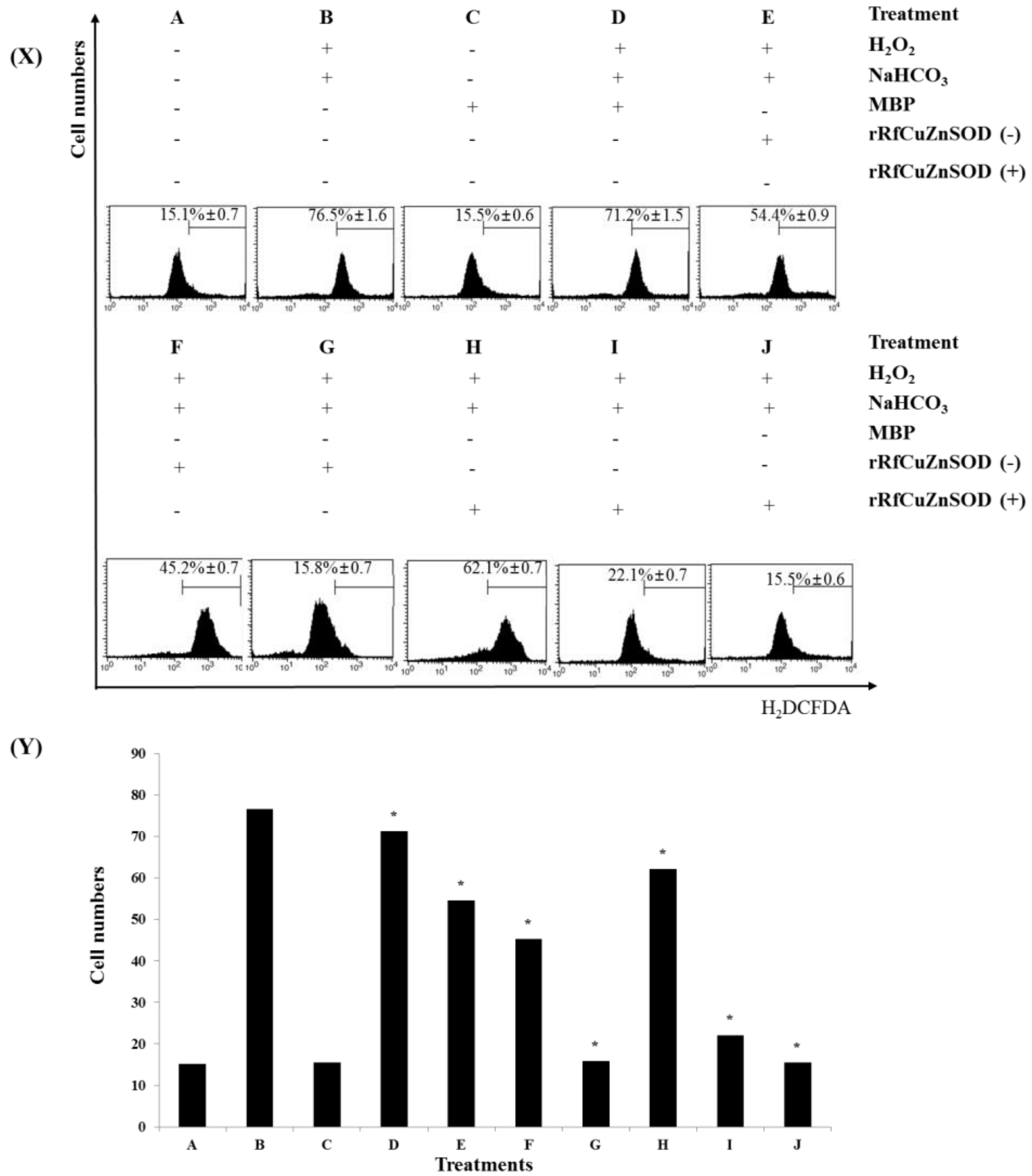

Figure 8. H_2O_2 scavenging activity of (A) rShCuZnSOD and (B) rRfCuZnSOD in the presence of HCO_3^-. (X) Mean cell numbers that expressed the intracellular H_2O_2 level after stained with H_2DCFDA. The treatments are as follows: (A) control cells, (B) 20 mM $NaHCO_3$ + 500 µmol H_2O_2, (C) 100 µg/mL of MBP, (D) 100 µg/mL of MBP + 20 mM $NaHCO_3$ + 500 µmol of H_2O_2, (E) 25 µg/mL of rCuZnSOD + 20 mM $NaHCO_3$ + 500 µmol of H_2O_2, (F) 50 µg/mL of rCuZnSOD + 20 mM $NaHCO_3$ + 500 µmol of H_2O_2 and (G) 100 µg/mL of rCuZnSOD + 20 mM $NaHCO_3$ + 500 µmol of H_2O_2, (H) 25 µg/mL of rCuZnSOD (+ metal) + 20 mM $NaHCO_3$ + 500 µmol of H_2O_2, (I) 50 µg/mL of rCuZnSOD (+ metal) + 20 mM $NaHCO_3$ + 500 µmol of H_2O_2, (J) 100 µg/mL of rCuZnSOD (+ metal) + 20 mM $NaHCO_3$ + 500 µmol of H_2O_2. (Y) Average cell numbers corresponding to each treatment (N = 3; $P < 0.05$). "*" indicates significant difference of the control and treatment.

Briefly, the H_2DCFDA was oxidized in to 2'7'-dichlorofluorescein by intracellular H_2O_2 (ROS), and then the fluorescence was detected by flow cytometer. Present flow cytometry results revealed that the intracellular ROS level was reduced in the presence of rCuZnSODs in a dose dependent manner. Briefly, the rCuZnSOD was reacting with the external H_2O_2 and reduce the level of oxidative stress to the cells. Thereby, the generation of intracellular ROS (H_2O_2) could alter by the rCuZnSODs. In addition, metal supplemented rCuZnSOD lowered the intracellular ROS generation compared to the non-supplemented rCuZnSOD treated THP-1 cells *via* scavenging extracellular H_2O_2. It affirmed that Cu^{2+} and Zn^{2+} enhance the peroxidation activity of rCuZnSODs. Therefore, these results will evident the possible peroxidation activity of rCuZnSOD. However, further experiments are warranted to enhance the knowledge of CuZnSOD as a peroxidase.

3.4 Expression analysis of *CuZnSODs*

3.4.1 *Spatial mRNA expression*

The importance of *CuZnSOD* in seahorse physiology was determined by examining the tissue-specific mRNA expression profile of both *ShCuZnSOD* and *RfCuZnSOD*. Expression was observed in the fourteen different tissues sampled, although the level of expression varied. The highest level of expression of *ShCuZnSOD* mRNA was detected in blood cells, which showed a ~34-fold increase compared with skin (Fig. 9). Also, the intense expression of *RfCuZnSOD* was observed in the in blood (34.11-fold) and followed by in ovary (25.28-fold).

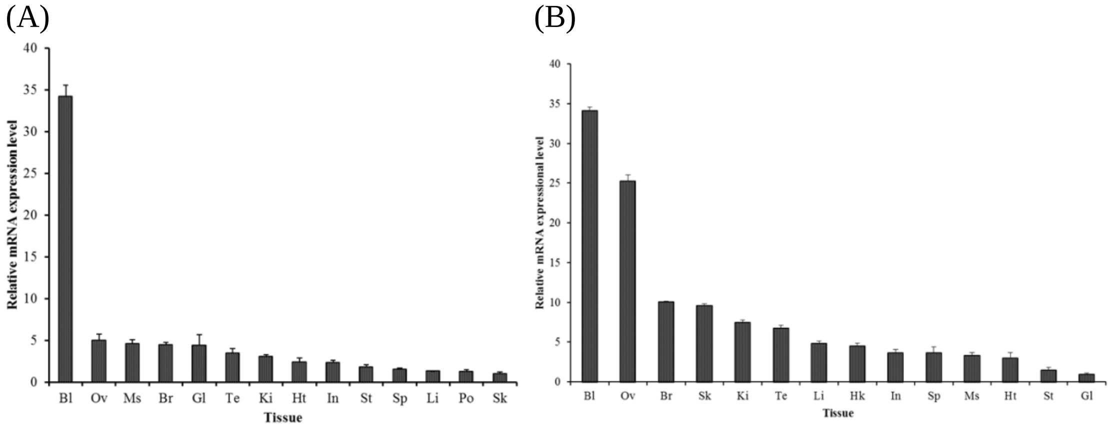

Figure 9. Relative levels of (A) *ShCuZnSOD* and (B) *RfCuZnSOD* mRNA in tissues of healthy animals. Blood (Bl), ovary (Ov), muscle (Ms), brain (Br), gill (Gl), testis (Te), kidney (Ki), heart (Ht), intestine (In), stomach (St), spleen (Sp), liver (Li), pouch (Po), skin (Sk), and head kidney (Hk). The tissues were collected from unchallenged seahorses and analyzed using qPCR. Data are presented as mean values (N = 3) with error bars representing standard deviation (SD).

The spatial distribution pattern of *CuZnSOD* mRNA has previously been determined in *O. fasciatus*, *Ruditapes philippinarum*, *Pseudosciaena crocea* and *Brassica campestris* besides reported that *CuZnSOD* is ubiquitously expressed in various tissues [13, 47, 48]. Likewise, in the current study, tissue expression profile of *ShCuZnSOD* and *RfCuZnSOD* revealed its constitutive expression in all the examined tissues with the highest expression in blood tissue which is known as an immune tissue and other tissues indicating its importance in immune regulation and other physiological functions respectively, which is yet to be studied. Among the fourteen tissues, blood tissue exhibited the extremely strong expression than in the other tissues. Lymphocytes are rich in blood which involve with the assisting of the defense mechanisms against the blood borne antigens. Phagocytosis, a defense mechanism is a cellular response that occurred to eliminate pathogens mainly in blood cells. This process can be stimulated to produce oxidative stress by generating ROS. Therefore, the CuZnSOD may express highly in blood tissues.

3.4.2 *Temporal mRNA expression*

The changes in transcription of *ShCuZnSOD* and *RfCuZnSOD* during the activation of host defenses to pathogenic invasion were investigated by measuring mRNA expression levels in blood. Significant induction of *ShCuZnSOD* against *E. tarda* was observed at 3 h p.i. where the significant induction against *S. iniae* was observed after 6 h p.i. Additionally a significant induction of *ShCuZnSOD* against poly I:C was observed at 24 h p.i. The highest level of *ShCuZnSOD* mRNA was present at 72 h post infection (Fig. 10). There was no any significant induction of *RfCuZnSOD* against *S. iniae*. However, a significant induction of *RfCuZnSOD* against LPS was observed at 12 h p.i. where a significant induction against poly I:C was observed at 6 h p.i.

(A) (B)

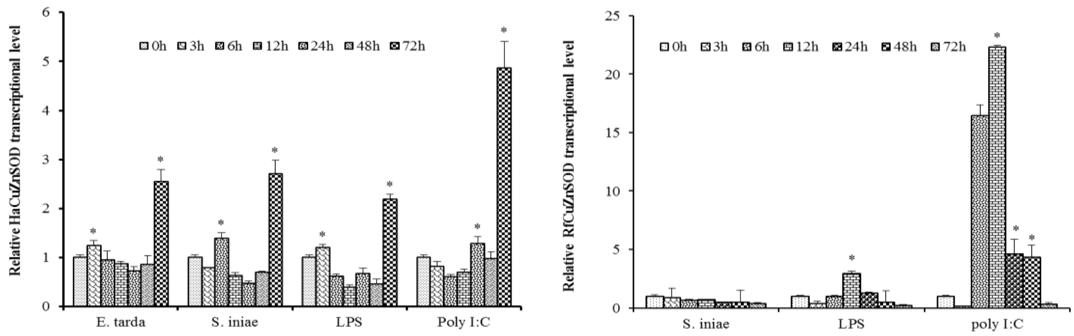

Figure 10. Transcriptional levels of (A) *ShCuZnSOD* and (B) *RfCuZnSOD* in blood after in vivo challenge with *E. tarda*, *S. iniae*, LPS and Poly I:C. "*" indicates significant difference of the control and treatment. Data are presented as mean values (N = 3) with error bars representing SD.

Furthermore, the expression of the *CuZnSOD* is known to be induced by many stimulants and with many live pathogens [13]. According to the results, late response was manifested by the *ShCuZnSOD* against the stimulants used. Since *ShCuZnSOD* is an antioxidant element, it might take certain time to give a response, because the formation of ROS after a pathogenic infection may take a little time. However, quiet different and varied results were observed in the *RfCuZnSOD* transcriptional pattern. Therefore, the *CuZnSOD* transcriptional pattern may be species specific. Further studies are warranted to be taken in order to explain the antioxidant role of the *CuZnSOD* after a pathogenic infection.

4. Chapter II

Molecular characterization of ShMnSOD and RfMnSOD while portraying their antioxidant functions

4.1 *In silico* analysis of MnSODs

4.1.1 *Delineation of sequence features and domain architecture*

Full length cDNA sequence corresponding to seahorse MnSOD was identified by homology screening which possesses an ORF of 669 bp coding for 223 amino acids (Fig. 11). Full length cDNA which is corresponded to rockfish MnSOD was also identified by homology screening which possesses an ORF of 678 bp coding for 225 aa. ShMnSOD has a molecular mass of 24.9 kDa and an isoelectric point of 7.75 where RfMnSOD has a predicted molecular mass of 25.10 kDa and a theoretical isoelectric point of 8.37. No signal peptide was found through the analysis, thus they might be intracellular proteins. According to the given results by MultiLoc tool, ShMnSOD and RfMnSOD were likely to be located in the mitochondria with an accuracy of 1. Mitochondria are the major producer of ROS from the electron transport chain, thus it could be directly attacked by these ROS [49]. However, these mMnSOD may play a crucial role *via* combating the ROS in the mitochondria. Additionally, it is stated that mMnSOD might crucial than cMnSOD in protecting the cells against oxidative stress [30]. Presence of two *N*-glycosylation sites affirms it as a glycoprotein similar to that of to the other orthologs [50, 51].

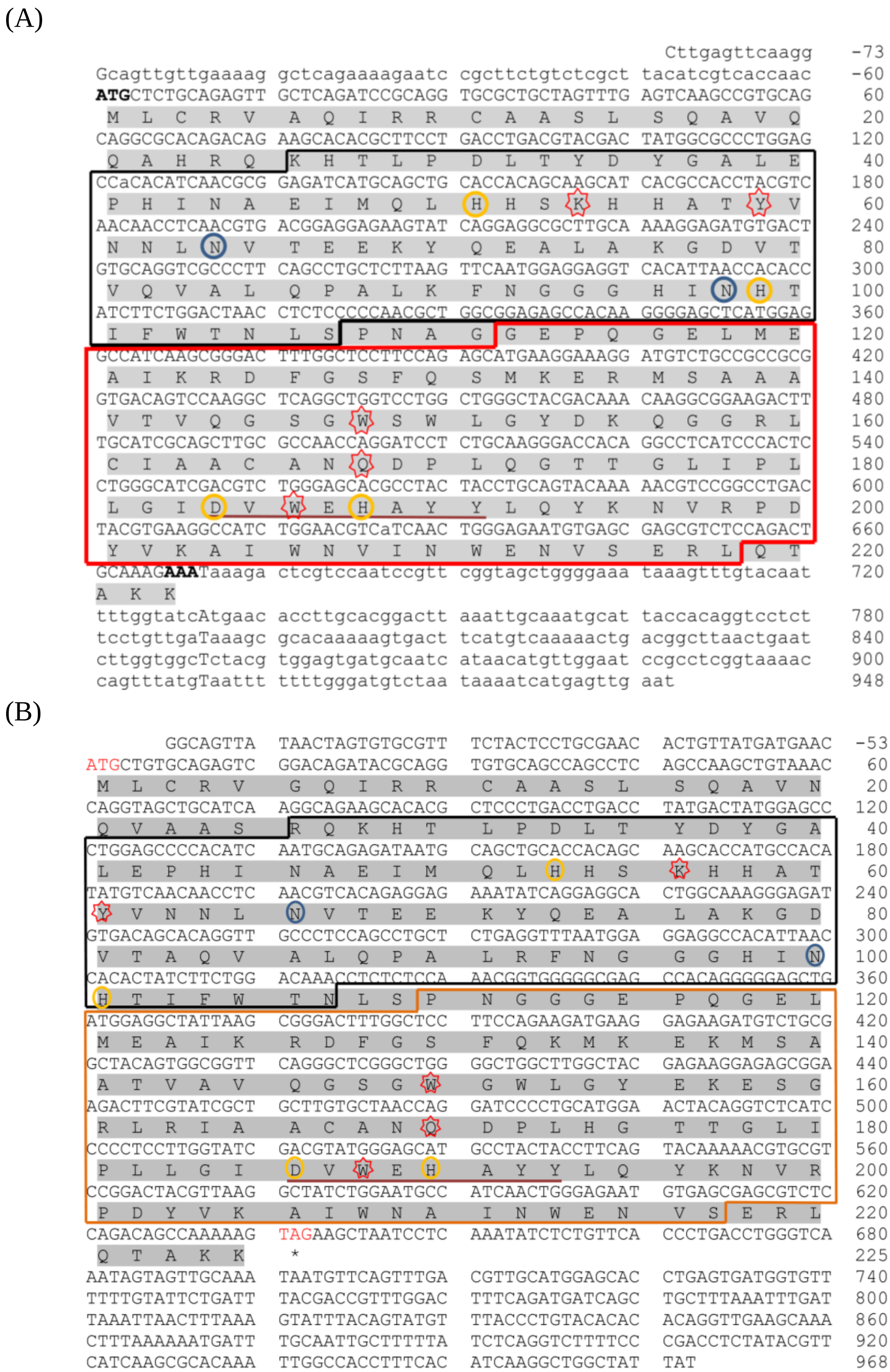

Figure 11. Domain architecture of (A) ShMnSOD and (B) RfMnSOD. SOD Fe-N domain is boxed in black where the SOD Fe-C is boxed in red. Manganese and iron superoxide dismutase signature is underlined with brown color. Mn^{+2} binding sites are round in orange circles and the active sites are round by red. Two predicted *N*-glycosylation sites are round by blue circles.

Two conservative domains including; Iron/Manganese SOD, C-terminal domain and Iron/Manganese SOD (SOD Fe-C domain), N-terminal domain (SOD Fe-N domain) were detected *via* the motif scan analyzer from both ShMnSOD and RfMnSOD. Moreover, the predicted metal binding sites for manganese ion were found at His^{51}, His^{99}, Asp^{184} and His^{188}. These binding sites may involve in mediating the catalytic function of ShMnSOD and RfMnSOD.

4.1.1 *Homology analysis*

In order to elucidate the conservation of the ShMnSOD and RfMnSOD throughout their evolution, homology analysis was conducted with bioinformatics tools. Clustal W pairwise alignment revealed the highest identity and similarity of ShMnSOD with *Opleganathus fasciatus* MnSOD (91.6% and 94.2% respectively) and followed by *Channa striata* MnSOD (89.8% and 93.3% respectively) (Fig. 12). ShMnSOD shows quiet high identity and similarity with the aves (~ 79% and 87.5% respctively), and mammalians (~ 77% and 84% respectively) as well. With respect to the RfMnSOD the highest identity was shared by *Oplegnathus faciatus* (97.3%) followed by *Sparus aurata* (96.4%) and *Epinephlus coioides* (96%). There similarities were 99.6, 98.7 and 98.2% respectively. Similar to ShMnSOD, RfMnSOD also showed high identity and similarities with the other aves (79.6%) and mammalian ortholgs (~77%). The multiple sequence alignment of ShMnSOD and RfMnSOD revealed that SOD Fe-N domain and the SOD Fe-C domain are highly conserved among the other selected orthologs (Fig. 13).

(A)

ShMnSOD			H. abdominalis	O. fasciatus	C. striata	P. olivaceus	K. marmoratus	M. amblycephala	H. molitrix	H. nobilis	H. mylodon	D. rerio	A. japonica	G. gallus	M. undulatus	H. sapiens	M. musculus	X. laevis	C. sapidus	A. irradians
Scientific Name	**Accesion No**		Identity%																	
Hippocampus abdominalis				91.6	89.8	88.9	87.6	85.3	85.3	84.8	84.4	84.4	83.9	79.0	78.1	77.4	77.0	76.2	68.6	63.3
Oplegnathus fasciatus	AFO64916		94.2		96.0	92.9	94.2	88.9	88.9	88.4	88.0	89.3	86.7	80.4	80.0	79.7	78.3	78.2	67.6	65.1
Channa striata	CCQ71732		93.8	100.0		93.3	92.4	87.6	87.6	87.1	86.2	88.4	87.1	80.9	80.0	78.4	77.9	77.7	68.0	64.6
Paralichthys olivaceus	BAJ79013		92.4	96.9	96.4		90.2	86.7	86.7	86.2	84.9	86.2	86.7	79.1	78.2	77.5	77.9	76.9	68.4	64.2
Kryptolebias marmoratus	AEM65187		92.4	98.7	98.7	96.0		89.3	89.3	88.9	87.6	87.6	84.0	80.0	78.7	77.1	75.7	79.0	67.6	64.6
Megalobrama amblycephala	AHK06412		90.6	94.7	95.6	92.9	94.2		97.8	98.2	96.0	95.1	83.5	80.8	81.3	81.3	80.5	81.3	70.4	67.7
Hypophthalmichthys molitrix	ADM86391		90.6	94.7	95.6	92.9	94.2	98.7		98.7	96.4	94.2	83.5	79.9	80.4	80.5	80.1	80.4	70.8	68.1
Hypophthalmichthys nobilis	ADM26563	Similarity%	90.6	94.7	95.6	92.9	94.2	98.7	99.1		96.9	94.6	83.0	79.9	80.4	81.3	80.1	80.4	70.8	68.6
Hemibarbus mylodon	ACR23311		90.2	94.2	94.7	92.0	93.3	97.3	97.8	97.8		93.3	83.5	78.6	79.0	80.5	80.1	79.0	71.0	67.7
Danio rerio	AAP34300		90.6	94.7	95.1	92.9	93.8	97.3	97.3	97.3	96.0		83.9	79.0	79.5	81.0	80.1	79.5	69.0	66.4
Anguilla japonica	BAL03637		91.9	95.1	94.7	93.3	93.8	93.8	93.8	93.8	93.8	94.2		78.6	77.7	78.0	77.0	79.1	68.5	63.4
Gallus gallus	AAK97214		87.9	88.9	88.9	88.0	88.0	89.7	89.3	89.3	88.4	87.9	89.3		92.4	83.5	84.0	81.7	70.2	63.2
Melopsittacus undulatus	AAO72712		87.1	88.0	88.4	87.6	87.6	89.7	89.3	89.3	88.4	87.1	89.7	96.9		83.6	82.7	83.9	70.2	66.4
Homo sapiens	CAA32502		85.7	87.1	88.0	86.2	86.2	87.5	87.9	87.9	88.4	87.9	90.1	90.2	91.1		89.6	81.3	69.8	65.8
Mus musculus	AAB60902		86.1	86.7	87.6	87.1	85.8	89.7	89.3	89.3	88.8	88.8	89.2	90.6	90.6	92.3		82.1	68.3	64.3
Xenopus laevis	AAQ63483		87.9	89.8	90.7	88.9	89.3	88.8	88.4	88.4	87.5	87.5	91.1	88.8	88.8	88.8	88.8		68.0	63.3
Callinectes sapidus	MAAF74770		79.4	79.1	79.6	80.9	77.3	79.0	79.0	79.0	79.5	78.6	81.0	80.4	79.9	80.2	79.3	79.0		66.1
Argopecten irradians	ABW98672		75.2	78.8	79.2	79.2	78.8	77.9	78.3	78.3	78.3	76.5	78.8	75.2	77.4	76.5	75.2	76.5	76.5	

(B)

RfMnSOD			S. schlegelii	O. fasciatus	S. aurata	E. coioides	R. canadum	T. obscurus	H. abdominalis	P. olivaceus	D. rerio	A. japonica	G. gallus	S. scrofa	H. sapiens	R. norvegicus	M. musculus	X. laevis	T. aestivum	C. sapidus	C. praedator	B. thermydron	P. clarkii	F. chinensis	M. rosenbergii
Scientific name	**Accession No**		Identity%																						
Sebastes schlegelii				97.3	96.4	96.0	95.1	93.4	91.6	91.6	88.4	85.8	79.6	79.3	78.9	78.9	77.9	76.9	50.4	49.0	48.3	47.6	45.8	45.6	45.5
Oplegnathus fasciatus	AFO64916		99.6		98.2	97.3	96.9	93.4	91.6	92.9	89.3	86.7	80.4	79.7	79.7	79.2	78.3	78.2	51.7	49.3	48.6	47.9	46.5	46.7	46.5
Sparus aurata	AFV39807		98.7	99.6		97.3	96.0	92.5	91.1	92.0	89.8	85.8	80.0	79.3	78.9	79.2	78.9	77.7	50.9	47.9	47.2	46.9	45.5	45.6	45.8
Epinephelus coioides	AAW29024		98.2	99.1	99.6		95.6	92.1	90.7	92.0	89.8	85.8	80.0	79.2	78.9	79.2	78.3	77.7	50.4	48.3	47.6	46.9	45.5	45.6	45.8
Rachycentron canadum	ABC71306		99.1	99.6	99.1	98.2		91.6	90.7	92.0	88.0	85.8	79.6	78.9	79.3	77.9	77.4	77.7	51.7	49.3	48.6	47.6	46.9	46.3	47.2
Takifugu obscurus	ABV24053		95.6	96.0	95.2	94.7	95.6		90.3	90.7	85.9	85.0	79.0	78.6	78.6	79.0	77.6	75.9	51.7	48.6	47.9	47.2	47.2	47.7	47.9
Hippocampus abdominalis			93.8	94.2	93.8	93.3	93.8	92.5		88.9	84.4	83.9	79.0	77.9	77.4	78.3	77.0	76.2	49.6	48.6	48.3	47.2	45.1	46.7	45.5
Paralichthys olivaceus	BAJ79013		96.0	96.9	96.4	96.0	96.0	93.0	92.4		86.2	86.7	79.1	77.9	77.5	78.3	77.9	76.9	51.3	47.2	47.2	47.2	45.5	46.3	46.2
Danio rerio	AAP34300		94.2	94.7	95.1	94.7	93.8	91.6	90.6	92.9		83.9	79.0	80.1	81.0	79.2	80.1	79.5	50.6	47.9	46.5	45.8	44.8	44.6	45.1
Anguilla japonica	BAL03637		94.7	95.1	94.7	94.2	94.2	92.5	91.9	93.3	94.2		78.6	77.9	78.0	77.5	77.0	79.1	53.0	46.9	45.8	44.4	45.8	43.9	45.1
Gallus gallus	AAK97214	Similarity%	88.4	88.9	88.4	88.4	88.9	87.7	87.9	88.0	87.9	89.3		84.8	83.5	84.4	84.0	81.7	52.6	45.8	48.3	46.2	46.9	46.0	47.2
Sus scrofa	NP_999292		88.4	88.9	88.0	87.1	88.4	87.7	87.4	88.0	88.8	91.0	92.0		91.9	90.5	91.0	81.7	52.3	46.5	47.6	47.2	46.5	46.0	46.2
Homo sapiens	CAA32502		86.7	87.1	86.7	86.2	87.1	86.8	85.7	86.2	87.9	90.1	90.2	94.1		88.3	89.6	81.3	51.5	46.5	46.9	47.6	47.6	46.0	46.2
Rattus norvegicus	NP_058747		88.4	87.6	88.0	87.6	87.6	86.8	87.9	89.3	88.4	88.3	90.6	93.7	91.9		94.6	81.7	52.6	45.5	47.2	46.5	44.8	45.3	44.1
Mus musculus	AAB60902		86.2	86.7	88.0	86.7	86.2	84.6	86.1	87.1	88.8	89.2	90.6	94.1	92.3	96.4		82.1	53.2	46.9	47.9	46.5	46.5	47.0	45.5
Xenopus laevis	AAQ63483		89.3	89.8	90.7	89.3	88.9	87.7	87.9	88.9	87.5	91.1	88.8	88.8	88.8	90.2	88.8		51.5	45.5	46.9	44.8	44.4	45.3	45.5
Triticum aestivum	AAX68501		64.5	65.4	64.9	64.9	64.9	64.9	63.6	64.9	64.5	65.4	64.1	64.9	64.5	65.4	65.8	65.4		37.2	36.8	35.9	37.8	37.8	37.5
Callinectes sapidus	AAF74771		59.4	59.8	59.4	58.7	58.7	59.1	59.1	58.0	58.0	58.4	56.3	57.3	56.6	55.6	56.3	56.3	49.3		89.9	87.4	78.3	78.7	77.3
Cyanagraea praedator	CAR85669		59.8	60.1	59.8	59.1	59.1	59.8	59.8	58.7	57.3	58.0	59.1	59.4	58.0	57.7	58.0	57.7	49.3	94.1		92.0	79.0	79.4	77.3
Bythograea thermydron	CAR85668		57.7	58.7	58.0	57.0	57.3	58.0	58.7	57.7	57.0	57.3	57.0	57.3	57.7	57.3	56.3	55.9	49.0	92.7	95.8		78.0	77.7	76.6
Procambarus clarkii	ABX44762		59.1	59.4	58.4	58.0	58.4	59.4	57.7	57.7	57.0	58.4	58.4	59.4	59.1	57.0	57.3	57	49.0	87.4	90.2	87.8		78.0	81.1
Fenneropenaeus chinensis	ACS49842		57.1	57.5	57.1	56.8	56.8	57.8	57.5	57.1	56.4	56.8	58.9	57.1	58.2	57.1	57.8	57.5	49.1	86.4	88.5	86.4	86.8		78.0
Macrobrachium rosenbergii	AAY79405		59.4	59.8	59.1	58.7	58.4	59.1	57.3	58.7	57.3	58.4	58.4	58.4	57.7	56.3	56.6	57.7	49.0	87.4	89.9	88.1	89.2	87.8	

Figure 12. Identity and similarity of (A) ShMnSOD and (B) RfMnSOD to other vertebrate and invertebrate counterparts.

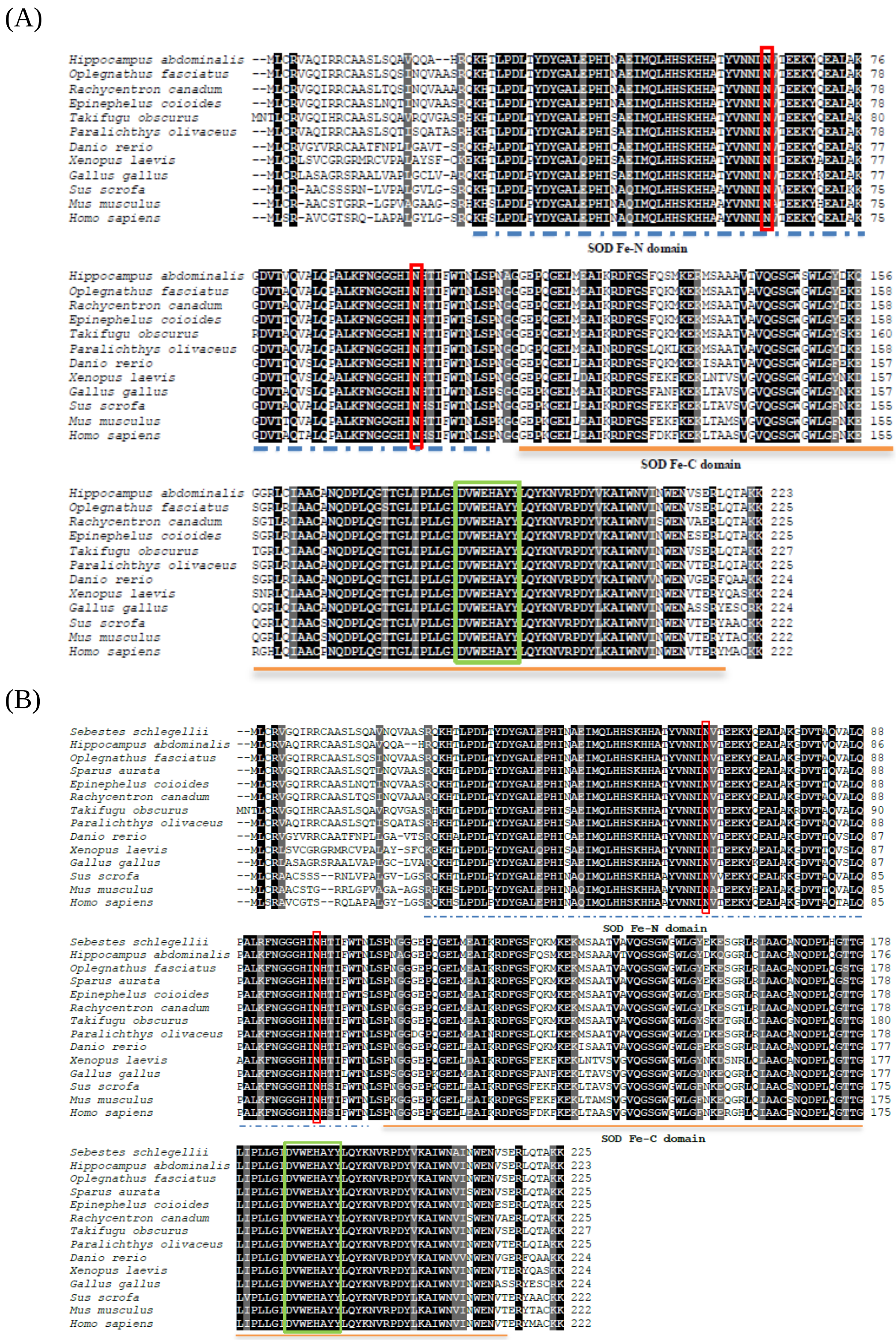

Figure 13. Multiple sequence alignment of (A) ShMnSOD and (B) RfMnSOD with vertebrate and invertebrate counterparts. Identical amino acids are indicated by black shading while partially conserved amino acids are indicated by grey shading. Conserved two *N*-glycosylation sites are boxed in red where the conserved Manganese and iron superoxide dismutase signature is boxed in green.

4.1.2 *Phylogenetic reconstruction*

The phylogenetic tree which was constructed with the known MnSOD orthologs exposed that, ShMnSOD closely cladded with *O. fasciatus* by further confirming the results of the pairwise comparison (Fig. 14). Fascinatingly, all the other orthologs of MnSOD which have been selected from different taxonomic groups have formed sub clusters by clustering together with the similar taxonomic orthologs thus; it is corresponded with conventional taxonomy. Additionally, it can be said that HaMnSOD and RfMnSOD are belonged to the fish MnSOD group as they have clustered together with the fish group. Taken together, highly conserved amino acids and the clustering pattern of two MnSODs would reflect that their structure and the function were likely to stabilize through the evolution.

(A)

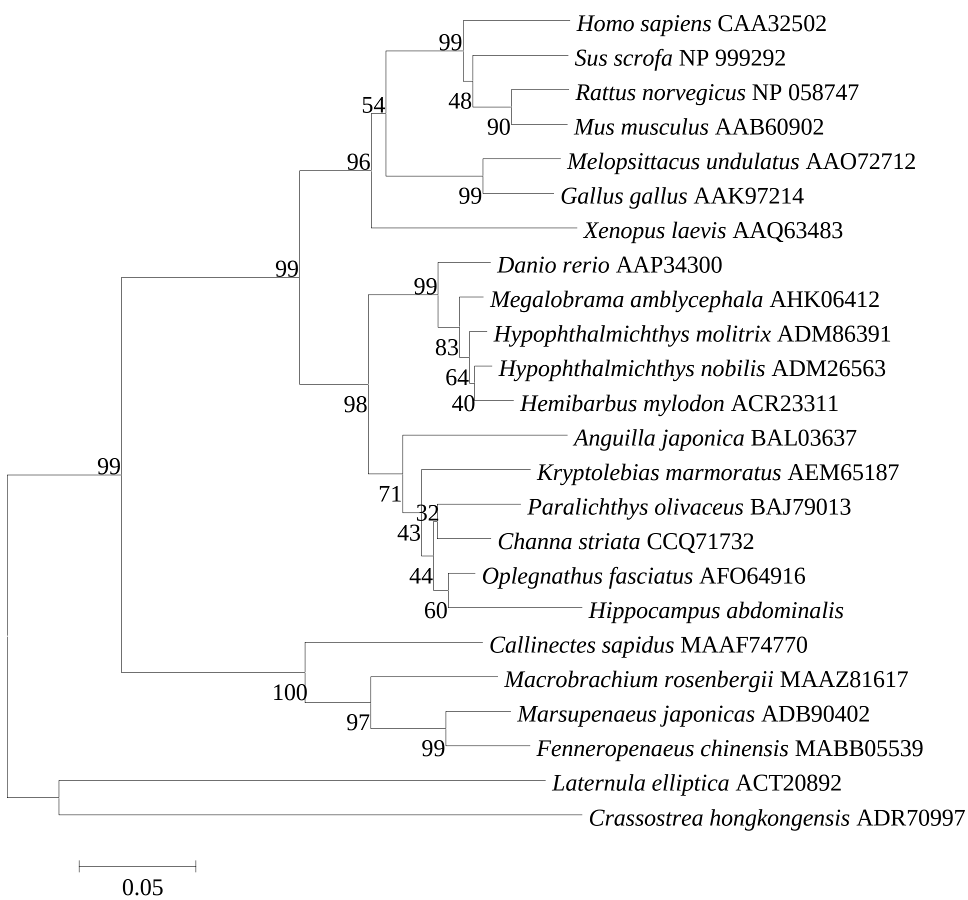

(B)

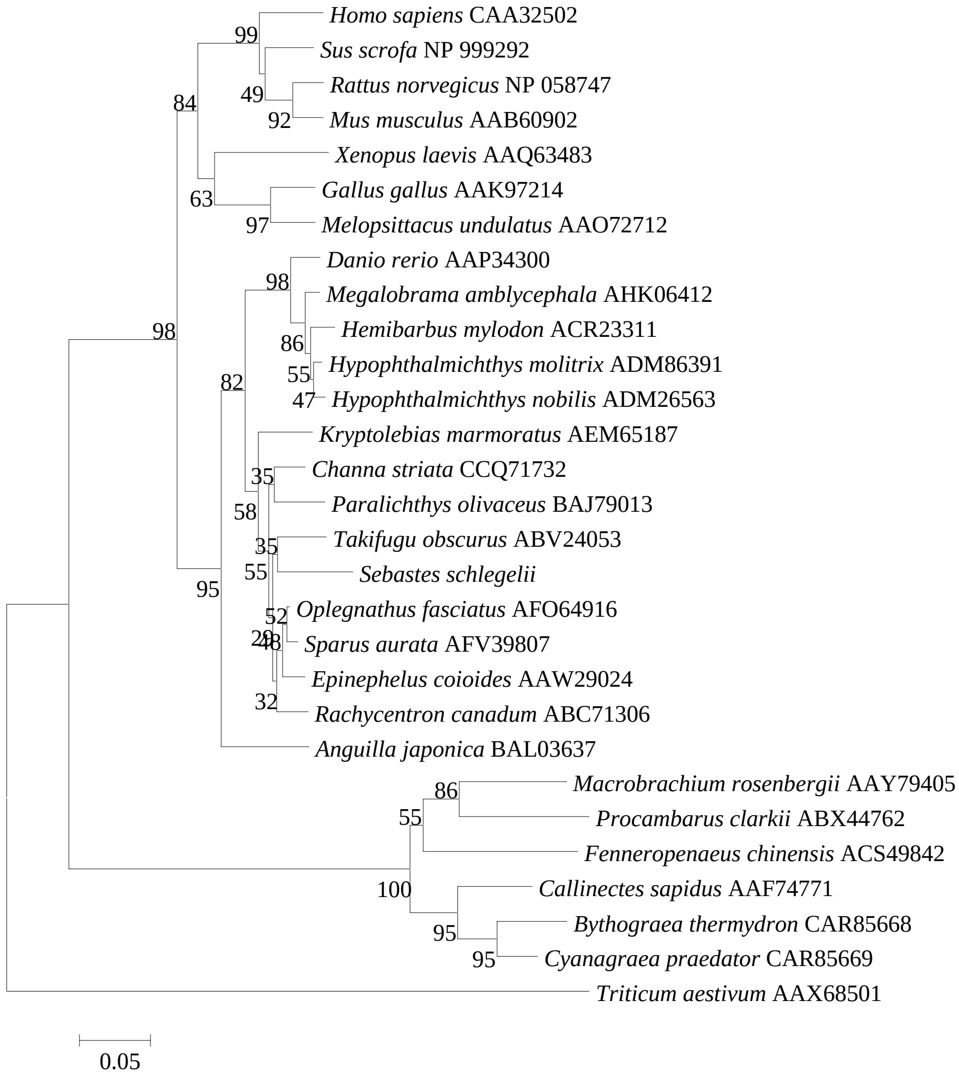

Figure 14. Unrooted phylogenetic tree depicting the relationship of (A) ShMnSOD and (B) RfMnSOD with its known orthologs. Numbers at the nodes indicate percent bootstrap confidence values derived from 5000 replications.

4.1.3 *Tertiary structure characterization*

Human MnSOD (PDB ID, 2adqB) template was used to determine the homodimer of ShMnSOD and RfMnSOD (Method: X-RAY DIFFRACTION, resolution: 2.4 A°, R-Value Free: 0.240, R-Value Work: 0.217) (Fig. 15). The Mn^{2+} binding sites and the active sites which are important for the stabilizing of the active site topology were demonstrated *via* the homology modeling [52]. Additionally, the structure of the ShMnSOD was more or less similar to that of to the rock bream MnSOD [51].

(A) (B)

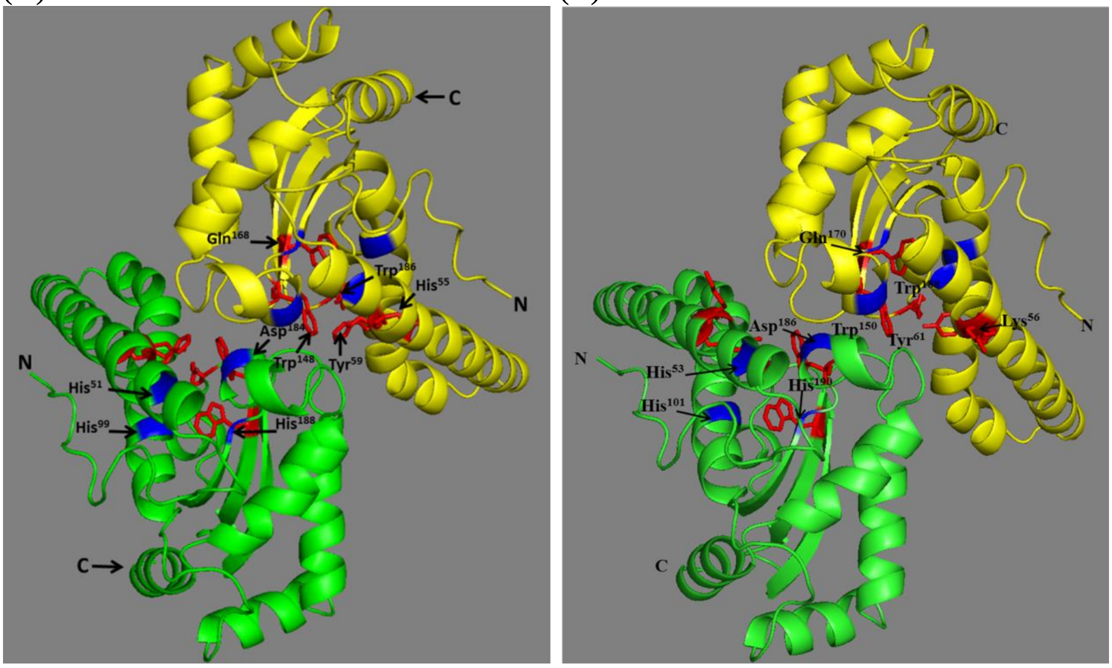

Figure 15. Predicted molecular model of the (A) ShMnSOD and (B) RfMnSOD tertiary structure. Mn^{2+} binding sites are denoted by the blue color. The active sites are marked in red color.

4.2 Antioxidant activity analysis of rMnSODs

4.2.1 *SOD assay with the effect of pH*

As previously described, the same xanthine/ xo assay was conducted in order to study the biochemical properties including optimum temperature and optimum pH of rShMnSOD and rRfMnSOD. The highest activity of rShMnSOD in scavenging superoxide radicals was observed at pH 9 (Fig. 16.1). Contritely, the highest SOD activity of rRfMnSOD was observed at pH 8. A significant activity of rShMnSOD was started from pH 7 and once the activity was reached to its optimum level the activity begins to reduce from pH 10. With respect to the rRfMnSOD its activity begins to reduce from pH 9. Both rMnSODs are more likely to be stable in the alkaline conditions than to that of to the acidic conditions as the other MnSODs [34, 53]. Additionally, at lower pHs the imidazole rings of Mn^{+2} liganding His residues might be protonated and lost its stability. Thereby, it is stated that the metal ligands may more stable in the alkaline conditions than in the acidic condition [54].

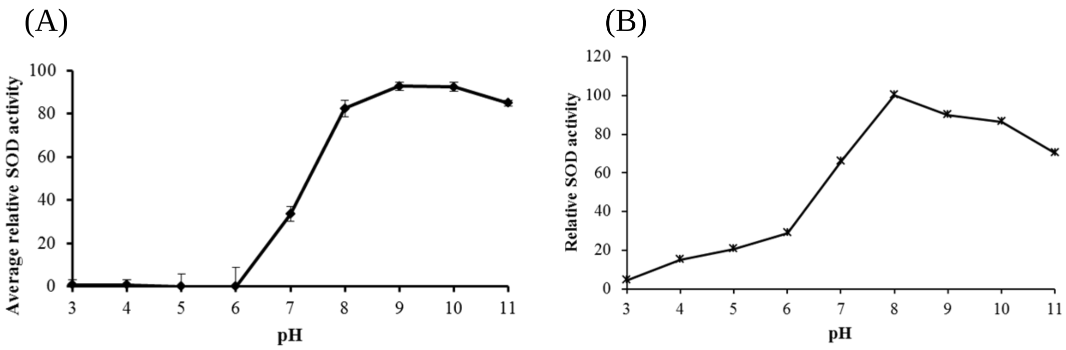

Figure 16.1 Xanthine/XO assay for the determination of optimum pH for (A) rShMnSOD and (B) rRfMnSOD.

4.2.2 *SOD assay with the effect of temperature*

The optimum temperature for its SOD activity of both rMnSODs was recorded at 25 ºC (Fig. 16.2). However significant SOD activity was shown in a wide range of temperature by both rShMnSOD and rRfMnSOD. Interestingly, for the rock bream MnSOD, optimum conditions are pH 9 and 20 ºC [51] where for the manila clam pH 9 and 20 ºC [47] are the optimum conditions.

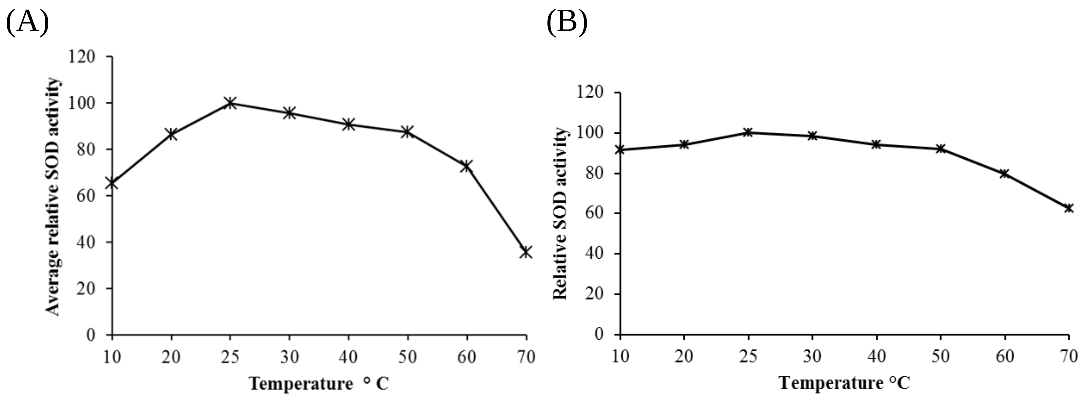

Figure 16.2 Xanthine/XO assay for the determination of optimum temperature for (A) rShMnSOD and (B) rRfMnSOD.

4.2.3 *Dose dependent antioxidant activity*

Then, we have examined the relative SOD activity of both rShMnSOD rRfMnSOD and checked their dose dependency (Fig. 16.3). According to the results, both rMnSODs showed high relative SOD activity affirming its high superoxide radicals scavenging ability compared to that of to the activity of rMBP. As well, rMBP doesn't show any significant activity. Moreover, the activity of both rMnSODs increased while increasing the concentration of rMnSODs revealing their dose dependency.

(A) (B)

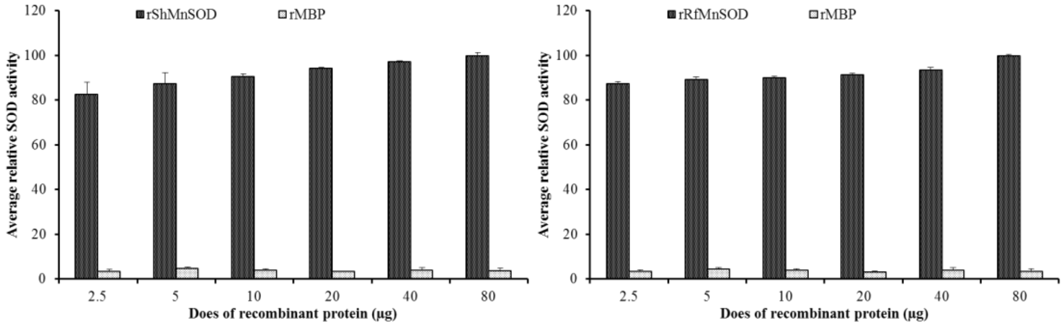

Figure 16.3 Xanthine/XO assay for the determination of dose dependent antioxidant activty (A) rShMnSOD and (B) rRfMnSOD.

4.2.4 *Effect of inhibitors*

The highest inhibition was observed with the incubation of KCN and followed by NaN_3 (Fig. 16.4). However, all the inhibitors were affected for the antioxidant activity of rShMnSOD and rRfMnSOD in different extents.

(A) (B)

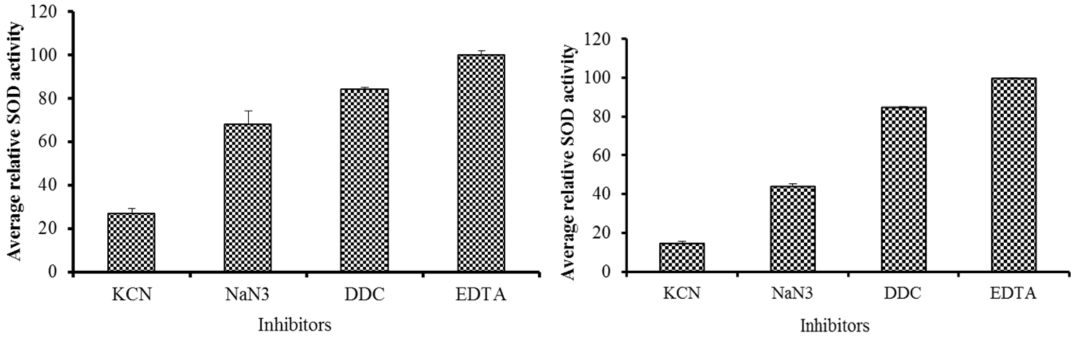

Figure 16.4 Effect of inhibitors on the antioxidant activity of (A) rShMnSOD and (B) rRfMnSOD.

4.3 Expression analysis of *MnSODs*

4.3.1 *Spatial mRNA expression*

A constitutive expression of *HaMnOSD* and *RfMnSOD* with variable levels was observed in all fourteen tissues examined in the tissue specific expressional analysis (Fig. 17). The highest expression was observed in the ovary and then followed by heart and brain in *ShMnSOD*. However, the highest expression of *RfMnSOD* was observed in blood and followed by ovary and skin. Generally; ovary, heart, brain and blood tissues are known as the tissues that required higher amount of energy for their metabolic functions. Also it is stated that large amount of mitochondria is connected with the cells that required higher amount of energy which have higher aerobic capacity [55, 56]. Germline cells also need more mitochondria than somatic cells since the requirement of energy is really high. Interestingly, a study has shown that the MnSOD has highly expressed in the mitochondria of the oocytes in *Dendrobaena veneta*. Therefore, this could be the reason for the highest expression of *ShMnSOD* in the ovary of seahorse, as it is the primary enzyme that can protect the cells from oxidative stress. Likewise, heart, brain and muscle are also required higher energy thus having high density of mitochondria and the same strategy applied on these tissues as well. In order to catalyze the dismutation of generated superoxides, high amount of MnSOD in those tissues is a requirement. Glycolysis, uncoupling of nitric oxide synthase, xanthine oxidase and NAD(P)H oxidases are some of the pathways that generate ROS in the kidney [57]. Therefore, having abundant MnSOD in the kidney tissues also an important for its strategy.

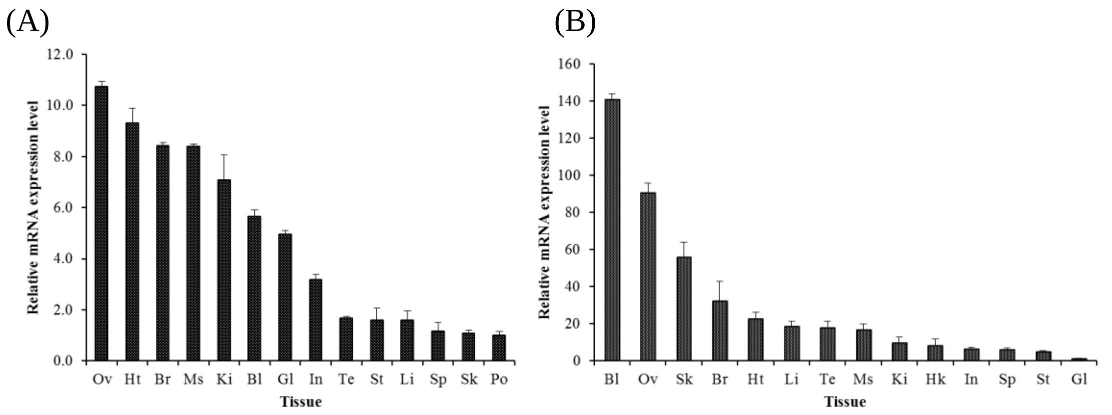

Figure 17. Relative levels of (A) *ShMnSOD* and (B) *RfMnSOD* mRNA in tissues of healthy animals. Blood (Bl), ovary (Ov), muscle (Ms), brain (Br), gill (Gl), testis (Te), kidney (Ki), heart (Ht), intestine (In), stomach (St), spleen (Sp), liver (Li), pouch (Po), skin (Sk), and head kidney (Hk). The tissues were collected from unchallenged seahorses and analyzed using qPCR. Data are presented as mean values (N = 3) with error bars representing standard deviation (SD).

4.3.2 *Temporal mRNA expression*

To further characterize the *ShMnSOD* and *RfMnSOD* in respect of immune related activities we have observed the transcriptional pattern of *ShMnSOD* and *RfMnSOD* mRNA against bacterial and viral stimulants. Additionally, we have selected blood as an immune tissue in order to observe the immune reactive response of *ShMnSOD* in the seahorse and *RfMnSOD* in rockfish. With respect to the qPCR results of *ShMnSOD*, a late response was observed against both bacterial and viral stimulants (Fig. 18). The strongest induction against each pathogenic stimulant was observed at 72 h p.i. Significant induction against *E. tarda* was observed at 3 h p.i. (25-fold) where the significant induction against *S. iniae* was observed after 6 h p.i. (1.5-fold). Moreover, *ShMnSOD* was significantly elevated at 72 h p.i. against LPS (1.7-fold) and at 24 h pi *ShMnSOD* was significantly elevated against poly I:C.

Contrast results were observed in the *RfMnSOD* expressional pattern against immune stimulants. Significant induction was only seen against LPS. The highest induction was observed at 6 h p.i. The transcriptional pattern therefore might be species specific in *MnSOD*.

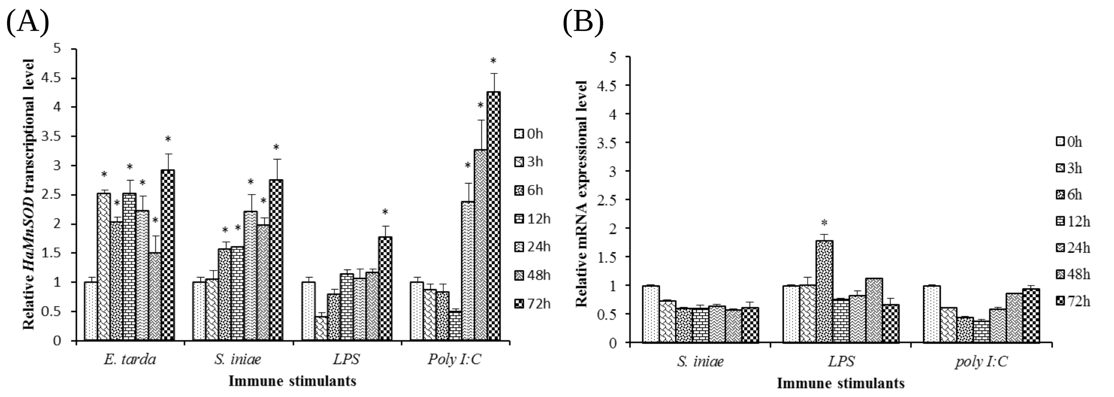

Figure 18. Transcriptional levels of (A) *ShMnSOD* and (B) *RfMnSOD* in blood after *in vivo* challenge with *E. tarda*, *S. iniae*, LPS and Poly I:C. "*" indicates significant difference of the control and treatment. Data are presented as mean values (N = 3) with error bars representing SD.

According to the previous studies, it is confirmed that MnSOD is a common stress responder which can be modulated by pathogenic stimulants, metal pollutants and environmental changes as well [53, 58-60]. Consistent with the results of the current study up-regulation of *MnSOD* was observed against bacterial stimuli [50, 61] as well as against viral stimuli [51].

5. Chapter III

Comparative analysis on structural and functional features of two different SODs; including CuZnSOD and MnSOD

CuZnSOD is a well-known blue copper protein, eythrocuprein, carried out the rapid catalytic dismutation of superoxide. CuZnSOD is a dimeric enzyme with each monomeric unit containing an active site of one copper and one zinc bridged by a histidine imidazole. The copper is bound by 3 additional histidines. The zinc is bound by two histidines and an aspartate in addition to the bridging imidazole. Copper is the redox-active metal, changing between the 2+/3+ oxidation states during catalysis, and zinc appears to play a role in overall enzyme stability and in facilitating a large pH independence in activity. Upon reduction of the $Cu^{2+}Zn^{2+}$SOD to $Cu^{+}Zn^{2+}$SOD, the bridging imidazole-copper coordination is lost, as is the bound water and the Cu^{+} shifts position and is three coordinate; otherwise both oxidized and reduced enzymes are generally structurally similar.

MnSODs are well conserved throughout evolution and across Kingdoms. MnSODs share a very high sequence and protein fold homology with FeSODs. MnSODs are found as dimers or tetramers, with a single manganese atom per subunit. Dimeric forms of MnSOD are typically found in bacteria, while Eukaryotes usually harbor tetrameric MnSOD. In bacteria, MnSOD is cytosolic, while in eukaryotes it is usually found in the mitochondrial matrix. Like other SODs, the MnSOD dismutation mechanism involves cycling between oxidized (Mn^{3+}) and reduced (Mn^{2+}) metal. The significant difference in the mechanism of MnSOD with that of other SODs is that the simple first-order disappearance of $O_2^{\bullet-}$ is not observed at sufficiently high ratios of [$O_2^{\bullet-}$]: [MnSOD], instead, there is a “burst phase” and a “zero-order” phase.

According to the *in silico* analysis of four SODs, ShCuZnSOD and RfCuZnSOD possess two copper/zinc superoxide dismutase signatures where ShMnSOD and RfMnSOD possess a manganese/ iron superoxide dismutase signature which facilitates their dismutation functions. Additionally, when compared to the ShCuZnSOD there are additional *N*-glycosylation sites and polypeptide binding sites in RfCuZnSOD. Through the 3D structural analysis it was found that both ShCuZnSOD and RfCuZnSOD was made up of 2 α helixes and a β-barrel motif of 8 β strands. The ShMnSOD and RfMnSOD were made up of 11 α helixes and 3 β strands. The structural conservation of these SOD members throughout the evolution was further supported by our alignment studies. The family signatures and the ion combining sites of these four SODs were completely conserved.

The functional studies revealed that the recombinant RfCuZnSOD possess a higher activity than that of to the recombinant ShCuZnSOD. The variation of the active sites may be the reason for this functional variation. As mentioned above the polypeptide binding sites of RfCuZnSOD was higher than in the ShCuZnSOD. The species specificity of CuZnSOD was highly demonstrated with the functional assays in this study. The inhibition rate of the SOD activity was also high in the rShCuZnSOD than to the rRfCuZnSOD. However, the antioxidant ability of the rShMnSOD was high than that of to the rRfMnSOD.

The transcriptional analysis of the four SODs demonstrated the ubiquitous feature where the expression was found in the each and every examined tissues but with different magnitudes. All these data collectively suggest that transcriptional profiles of SODs are subtype- and species dependent. In particular, differential expression of MnSOD was tissue-specific and proposed to be associated with relative content of mitochondria and oxidative load, as it is the principal antioxidant scavenger of ROS generated during aerobic respiration. The SODs are considered to be common stress-responsive elements of defense system whose mRNA expression could be modulated by various factors including environmental changes, chemical pollutants (heavy metals) and biological stimuli (pathogens). Our results indicated that these experimental injections significantly altered the transcription of all SODs in blood of challenged fish. In fact, the SOD expression patterns varied in terms of magnitude and kinetics with different challenging agents and the tissue type.

Conclusions

In the present study four SODs members have identified and characterized in terms of cDNA, functional assays and immune responsive transcriptional changes within the two teleost species; big belly seahorse; *Hippocampus abdominali* and, rockfish; *Sebastes schligelli*. Briefly, we have cloned the ShCuZnSOD, RfCuZnSOD, ShMnSOD and RfMnSOD which were found from an established cDNA library. The structural features then characterized with bioinformatics web-tools and software. Through the bioinformatics it was confirmed that all four sods were belonged to the eukaryotic enzymes and highly conserved with respect to the other orthologs. Resu;ts from the xanthine/XOD assay showed that they were functiones as antioxidant enzymes. MTT and flow cytometry analysis were used to study the peroxidation function of rShCuZnSOD and rRfCuZnSOD in the presence of HCO_3^-. Furthermore, employed experimental method provides complete and sound understanding of the immunological role of four sods as it summarized the mRNA expression of each gene upon diverse immune stimulants and pathogen challenges. Overall, we suggest that ShCuZnSOD, RfCuZnSOD, ShMnSOD and RfMnSOD are antioxidant gene encoding a protein with many crucial roles in the host denfense.

Reference

[1] H.J. Forman, M. Torres, Redox signaling in macrophages, Mol Aspects Med 22(4-5) (2001) 189-216.

[2] B.M. Babior, R.S. Kipnes, J.T. Curnutte, Biological defense mechanisms. The production by leukocytes of superoxide, a potential bactericidal agent, J Clin Invest 52(3) (1973) 741-4.

[3] W.A. Pryor, K.N. Houk, C.S. Foote, J.M. Fukuto, L.J. Ignarro, G.L. Squadrito, K.J. Davies, Free radical biology and medicine: it's a gas, man!, Am J Physiol Regul Integr Comp Physiol 291(3) (2006) R491-511.

[4] E. Cadenas, Basic mechanisms of antioxidant activity, Biofactors 6(4) (1997) 391-7.

[5] I. Fridovich, Biological effects of the superoxide radical, Arch Biochem Biophys 247(1) (1986) 1-11.

[6] D.D. Mruk, B. Silvestrini, M.Y. Mo, C.Y. Cheng, Antioxidant superoxide dismutase - a review: its function, regulation in the testis, and role in male fertility, Contraception 65(4) (2002) 305-11.

[7] M. Angelova, P. Dolashka-Angelova, E. Ivanova, J. Serkedjieva, L. Slokoska, S. Pashova, R. Toshkova, S. Vassilev, I. Simeonov, H.J. Hartmann, S. Stoeva, U. Weser, W. Voelter, A novel glycosylated Cu/Zn-containing superoxide dismutase: production and potential therapeutic effect, Microbiology 147(Pt 6) (2001) 1641-50.

[8] S.L. Williams, N. Janetski, J. Abbott, S. Blankenhorn, B. Cheng, R.E. Crafton, S.O. Hameed, S. Rapi, D. Trockel, Ornamental marine species culture in the coral triangle: seahorse demonstration project in the Spermonde Islands, Sulawesi, Indonesia, Environ Manage 54(6) (2014) 1342-55.

[9] M. Droege, B. Hill, The Genome Sequencer FLX System--longer reads, more applications, straight forward bioinformatics and more complete data sets, J Biotechnol 136(1-2) (2008) 3-10.

[10] G.I. Godahewa, N.C. Perera, N. Umasuthan, Q. Wan, I. Whang, J. Lee, Molecular characterization and expression analysis of B cell activating factor from rock bream (Oplegnathus fasciatus), Dev Comp Immunol 55 (2016) 1-11.

[11] M.M. Bradford, A rapid and sensitive method for the quantitation of microgram quantities of protein utilizing the principle of protein-dye binding, Anal Biochem 72 (1976) 248-54.

[12] C. Beauchamp, I. Fridovich, Superoxide dismutase: improved assays and an assay applicable to acrylamide gels, Anal Biochem 44(1) (1971) 276-87.

[13] N. Umasuthan, S.D. Bathige, W.S. Thulasitha, W. Qiang, B.S. Lim, J. Lee, Characterization of rock bream (Oplegnathus fasciatus) cytosolic Cu/Zn superoxide dismutase in terms of molecular structure, genomic arrangement, stress-induced mRNA expression and antioxidant function, Comp Biochem Physiol B Biochem Mol Biol 176 (2014) 18-33.

[14] D.M. Spinner, MTT growth assays in ovarian cancer, Methods Mol Med 39 (2001) 175-7.

[15] G.I. Godahewa, W.D. Wickramaarachchi, I. Whang, S.D. Bathige, B.S. Lim, C.Y. Choi, M. De Zoysa, J.K. Noh, J. Lee, Two carboxypeptidase counterparts from rock bream (Oplegnathus fasciatus): molecular characterization, genomic arrangement and immune responses upon pathogenic stresses, Vet Immunol Immunopathol 162(3-4) (2014) 180-91.

[16] K.J. Livak, T.D. Schmittgen, Analysis of relative gene expression data using real-time quantitative PCR and the 2(-Delta Delta C(T)) Method, Methods 25(4) (2001) 402-8.

[17] M. Li, Y. Zheng, H. Liang, L. Zou, J. Sun, Y. Zhang, F. Qin, S. Liu, Z. Wang, Molecular cloning and characterization of cat, gpx1 and Cu/Zn-sod genes in pengze crucian carp (Carassius auratus var. Pengze) and antioxidant enzyme modulation induced by hexavalent chromium in juveniles, Comp Biochem Physiol C Toxicol Pharmacol 157(3) (2013) 310-21.

[18] W. Xiong, L. Bai, R.U. Muhammad, M. Zou, Y. Sun, Molecular cloning, characterization of copper/zinc superoxide dismutase and expression analysis of stress-responsive genes from Eisenia fetida against dietary zinc oxide, Comp Biochem Physiol C Toxicol Pharmacol 155(2) (2012) 416-22.

[19] N. Chakravarthy, K. Aravindan, N. Kalaimani, S.V. Alavandi, M. Poornima, T.C. Santiago, Intracellular Copper Zinc Superoxide dismutase (icCuZnSOD) from Asian seabass (Lates calcarifer): molecular cloning, characterization and gene expression with reference to Vibrio anguillarum infection, Dev Comp Immunol 36(4) (2012) 751-5.

[20] V. Kumaresan, A.J. Gnanam, M. Pasupuleti, M.V. Arasu, N.A. Al-Dhabi, R. Harikrishnan, J. Arockiaraj, Comparative analysis of CsCu/ZnSOD defense role by

molecular characterization: gene expression-enzyme activity-protein level, Gene 564(1) (2015) 53-62.

[21] M.C. Rubio, M. Becana, S. Kanematsu, T. Ushimaru, E.K. James, Immunolocalization of antioxidant enzymes in high-pressure frozen root and stem nodules of Sesbania rostrata, New Phytol 183(2) (2009) 395-407.

[22] L.Y. Chang, J.W. Slot, H.J. Geuze, J.D. Crapo, Molecular immunocytochemistry of the CuZn superoxide dismutase in rat hepatocytes, J Cell Biol 107(6 Pt 1) (1988) 2169-79.

[23] J.M. Li, Y.L. Su, X.L. Gao, J. He, S.S. Liu, X.W. Wang, Molecular characterization and oxidative stress response of an intracellular Cu/Zn superoxide dismutase (CuZnSOD) of the whitefly, Bemisia tabaci, Arch Insect Biochem Physiol 77(3) (2011) 118-33.

[24] J.A. Tainer, E.D. Getzoff, K.M. Beem, J.S. Richardson, D.C. Richardson, Determination and analysis of the 2 A-structure of copper, zinc superoxide dismutase, J Mol Biol 160(2) (1982) 181-217.

[25] R. Fukuhara, T. Tezuka, T. Kageyama, Structure, molecular evolution, and gene expression of primate superoxide dismutases, Gene 296(1-2) (2002) 99-109.

[26] D.S. Shin, M. Didonato, D.P. Barondeau, G.L. Hura, C. Hitomi, J.A. Berglund, E.D. Getzoff, S.C. Cary, J.A. Tainer, Superoxide dismutase from the eukaryotic thermophile Alvinella pompejana: structures, stability, mechanism, and insights into amyotrophic lateral sclerosis, J Mol Biol 385(5) (2009) 1534-55.

[27] D. Bordo, K. Djinovic, M. Bolognesi, Conserved patterns in the Cu,Zn superoxide dismutase family, J Mol Biol 238(3) (1994) 366-86.

[28] M.W. Smith, R.F. Doolittle, A comparison of evolutionary rates of the two major kinds of superoxide dismutase, J Mol Evol 34(2) (1992) 175-84.

[29] F. Rodriguez-Trelles, R. Tarrio, F.J. Ayala, Erratic overdispersion of three molecular clocks: GPDH, SOD, and XDH, Proc Natl Acad Sci U S A 98(20) (2001) 11405-10.

[30] Q. Zhang, F. Li, B. Wang, J. Zhang, Y. Liu, Q. Zhou, J. Xiang, The mitochondrial manganese superoxide dismutase gene in Chinese shrimp Fenneropenaeus chinensis: cloning, distribution and expression, Dev Comp Immunol 31(5) (2007) 429-40.

[31] Z.W. Zhang, Z. Li, H.W. Liang, L. Li, X.Z. Luo, G.W. Zou, Molecular cloning and differential expression patterns of copper/zinc superoxide dismutase and

manganese superoxide dismutase in Hypophthalmichthys molitrix, Fish Shellfish Immunol 30(2) (2011) 473-9.
[32] D. Ni, L. Song, Q. Gao, L. Wu, Y. Yu, J. Zhao, L. Qiu, H. Zhang, F. Shi, The cDNA cloning and mRNA expression of cytoplasmic Cu, Zn superoxide dismutase (SOD) gene in scallop Chlamys farreri, Fish Shellfish Immunol 23(5) (2007) 1032-42.
[33] C.F. Ken, C.T. Lin, J.F. Shaw, J.L. Wu, Characterization of fish Cu/Zn-superoxide dismutase and its protection from oxidative stress, Mar Biotechnol (NY) 5(2) (2003) 167-73.
[34] Y. Bao, L. Li, F. Xu, G. Zhang, Intracellular copper/zinc superoxide dismutase from bay scallop Argopecten irradians: its gene structure, mRNA expression and recombinant protein, Fish Shellfish Immunol 27(2) (2009) 210-20.
[35] K. Guruprasad, B.V. Reddy, M.W. Pandit, Correlation between stability of a protein and its dipeptide composition: a novel approach for predicting in vivo stability of a protein from its primary sequence, Protein Eng 4(2) (1990) 155-61.
[36] K. Kulthanan, P. Nuchkull, S. Varothai, The pH of water from various sources: an overview for recommendation for patients with atopic dermatitis, Asia Pac Allergy 3(3) (2013) 155-60.
[37] E.D. Getzoff, J.A. Tainer, P.K. Weiner, P.A. Kollman, J.S. Richardson, D.C. Richardson, Electrostatic recognition between superoxide and copper, zinc superoxide dismutase, Nature 306(5940) (1983) 287-90.
[38] E. Argese, P. Viglino, G. Rotilio, M. Scarpa, A. Rigo, Electrostatic control of the rate-determining step of the copper, zinc superoxide dismutase catalytic reaction, Biochemistry 26(11) (1987) 3224-8.
[39] H.H. Xu, H. Ma, B.Q. Hu, D.B. Lowrie, X.Y. Fan, C.G. Wen, Molecular cloning, identification and functional characterization of a novel intracellular Cu-Zn superoxide dismutase from the freshwater mussel Cristaria plicata, Fish Shellfish Immunol 29(4) (2010) 615-22.
[40] J.V. Bannister, W.H. Bannister, R.C. Bray, E.M. Fielden, P.B. Roberts, G. Rotilio, The superoxide dismutase activity of human erythrocuprein, FEBS Lett 32(2) (1973) 303-6.
[41] I. Fridovich, Superoxide radical and superoxide dismutases, Annu Rev Biochem 64 (1995) 97-112.

[42] R.H. Gottfredsen, U.G. Larsen, J.J. Enghild, S.V. Petersen, Hydrogen peroxide induce modifications of human extracellular superoxide dismutase that results in enzyme inhibition, Redox Biol 1 (2013) 24-31.
[43] S. Sankarapandi, J.L. Zweier, Bicarbonate is required for the peroxidase function of Cu, Zn-superoxide dismutase at physiological pH, J Biol Chem 274(3) (1999) 1226-32.
[44] G.I. Godahewa, Y. Kim, S.H. Dananjaya, R.G. Jayasooriya, J.K. Noh, J. Lee, M. De Zoysa, Mitochondrial peroxiredoxin 3 (Prx3) from rock bream (Oplegnathus fasciatus): immune responses and role of recombinant Prx3 in protecting cells from hydrogen peroxide induced oxidative stress, Fish Shellfish Immunol 43(1) (2015) 131-41.
[45] S.R. Powell, The antioxidant properties of zinc, J Nutr 130(5S Suppl) (2000) 1447S-54S.
[46] M.Y. Jing, J.Y. Sun, N.T. Zi, W. Sun, L.C. Qian, X.Y. Weng, Effects of zinc on hepatic antioxidant systems and the mRNA expression levels assayed by cDNA microarrays in rats, Ann Nutr Metab 51(4) (2007) 345-51.
[47] N. Umasuthan, S.D. Bathige, K.S. Revathy, Y. Lee, I. Whang, C.Y. Choi, H.C. Park, J. Lee, A manganese superoxide dismutase (MnSOD) from Ruditapes philippinarum: comparative structural- and expressional-analysis with copper/zinc superoxide dismutase (Cu/ZnSOD) and biochemical analysis of its antioxidant activities, Fish Shellfish Immunol 33(4) (2012) 753-65.
[48] H. Liu, J. He, C. Chi, Y. Gu, Identification and analysis of icCu/Zn-SOD, Mn-SOD and ecCu/Zn-SOD in superoxide dismutase multigene family of Pseudosciaena crocea, Fish Shellfish Immunol 43(2) (2015) 491-501.
[49] F.Q. Liang, B.F. Godley, Oxidative stress-induced mitochondrial DNA damage in human retinal pigment epithelial cells: a possible mechanism for RPE aging and age-related macular degeneration, Exp Eye Res 76(4) (2003) 397-403.
[50] D. Zhang, S. Cui, H. Guo, S. Jiang, Genomic structure, characterization and expression analysis of a manganese superoxide dismutase from pearl oyster Pinctada fucata, Dev Comp Immunol 41(4) (2013) 484-90.
[51] N. Umasuthan, K.S. Revathy, S.D. Bathige, B.S. Lim, M.A. Park, I. Whang, J. Lee, A manganese superoxide dismutase with potent antioxidant activity identified from Oplegnathus fasciatus: genomic structure and transcriptional characterization, Fish Shellfish Immunol 34(1) (2013) 23-37.

[52] J. Porta, A. Vahedi-Faridi, G.E. Borgstahl, Structural analysis of peroxide-soaked MnSOD crystals reveals side-on binding of peroxide to active-site manganese, J Mol Biol 399(3) (2010) 377-84.

[53] H. Park, I.Y. Ahn, J.K. Lee, S.C. Shin, J. Lee, E.J. Choy, Molecular cloning, characterization, and the response of manganese superoxide dismutase from the Antarctic bivalve Laternula elliptica to PCB exposure, Fish Shellfish Immunol 27(3) (2009) 522-8.

[54] A. Dolashki, R. Abrashev, S. Stevanovic, L. Stefanova, S.A. Ali, L. Velkova, R. Hristova, M. Angelova, W. Voelter, B. Devreese, J. Van Beeumen, P. Dolashka-Angelova, Biochemical properties of Cu/Zn-superoxide dismutase from fungal strain Aspergillus niger 26, Spectrochim Acta A Mol Biomol Spectrosc 71(3) (2008) 975-83.

[55] C.D. Moyes, B.J. Battersby, S.C. Leary, Regulation of muscle mitochondrial design, J Exp Biol 201(Pt 3) (1998) 299-307.

[56] P. de Paz, A. Zapata, J. Renau-Piqueras, F. Miragall, Morphological differentiation of mitochondria in the early chick embryo: a stereological analysis, Histol Histopathol 1(2) (1986) 197-201.

[57] J.M. Forbes, M.T. Coughlan, M.E. Cooper, Oxidative stress as a major culprit in kidney disease in diabetes, Diabetes 57(6) (2008) 1446-54.

[58] G.A. Visner, W.C. Dougall, J.M. Wilson, I.A. Burr, H.S. Nick, Regulation of manganese superoxide dismutase by lipopolysaccharide, interleukin-1, and tumor necrosis factor. Role in the acute inflammatory response, J Biol Chem 265(5) (1990) 2856-64.

[59] Q. Wang, Z. Yuan, H. Wu, F. Liu, J. Zhao, Molecular characterization of a manganese superoxide dismutase and copper/zinc superoxide dismutase from the mussel Mytilus galloprovincialis, Fish Shellfish Immunol 34(5) (2013) 1345-51.

[60] K.Y. Kim, S.Y. Lee, Y.S. Cho, I.C. Bang, K.H. Kim, D.S. Kim, Y.K. Nam, Molecular characterization and mRNA expression during metal exposure and thermal stress of copper/zinc- and manganese-superoxide dismutases in disk abalone, Haliotis discus discus, Fish Shellfish Immunol 23(5) (2007) 1043-59.

[61] L. Zheng, B. Wu, Z. Liu, J. Tian, T. Yu, L. Zhou, X. Sun, A. Yang, A manganese superoxide dismutase (MnSOD) from ark shell, Scapharca broughtonii: Molecular characterization, expression and immune activity analysis, Fish Shellfish Immunol 45(2) (2015) 656-65.